

NGR-10-005-127

A METHOD FOR CALCULATING THE  
INDUCED PRESSURE DISTRIBUTION ASSOCIATED  
WITH A JET IN A CROSSFLOW

*date due*



By

William E. Dietz, Jr.

(NASA-CR-146434) A METHOD FOR CALCULATING  
THE INDUCED PRESSURE DISTRIBUTION ASSOCIATED  
WITH A JET IN A CROSSFLOW M.S. Thesis  
(Florida Univ.) 82 p HC \$5.00 CSCL 20D

N76-19367

Unclas  
G3/34 07364

A THESIS PRESENTED TO THE GRADUATE COUNCIL OF  
THE UNIVERSITY OF FLORIDA  
IN PARTIAL FULFILLMENT OF THE REQUIREMENTS FOR THE  
DEGREE OF MASTER OF SCIENCE

UNIVERSITY OF FLORIDA

1975

## ACKNOWLEDGEMENTS

Financial support for this study was provided by NASA Grant NGR 10-005-127 under the technical direction of Mr. R. J. Margason, NASA Langley Research Center, Hampton, Virginia. The author wishes to express his appreciation to Dr. Richard L. Fearn and Robert P. Weston for their guidance and aid during the preparation of this thesis. The author also wishes to thank Karen Fleck, whose assistance in the completion of this thesis is greatly appreciated.

## TABLE OF CONTENTS

Acknowledgements	ii
List of Figures	iv
Symbols	vi
Abstract	viii
Introduction	1
Literature Review	4
Formulation of Problem	11
Results	19
Conclusion	23
Figures	24
Appendices	45
References	72
Biographical Sketch	74

## LIST OF FIGURES

1. Sketch of VTOL Aircraft Transitioning from Hovering to  
Horizontal Flight
2. Geometry of Vortex Models
3. Arrangement of Singularity Distributions in the Model
4. Tunnel and Field Point Coordinate Systems
5. Comparison of Model Results with Experimental Pressure  
Coefficients for Zero Entrainment ( $0^\circ < \theta < 90^\circ$ )
6. Comparison of Model Results with Experimental Pressure  
Coefficients for Zero Entrainment ( $105^\circ < \theta < 180^\circ$ )
7. Comparison of Model Results with Experimental Pressure  
Coefficients for Zero Entrainment ( $.58 < r/D < 1.00$ )
8. Comparison of Model Results with Experimental Pressure  
Contours for Zero Entrainment
9. Comparison of Model Results with Experimental Pressure  
Coefficients for  $E=0.6$  ( $0^\circ < \theta < 90^\circ$ )
10. Comparison of Model Results with Experimental Pressure  
Coefficients for  $E=0.6$  ( $105^\circ < \theta < 180^\circ$ )
11. Comparison of Model Results with Experimental Pressure  
Coefficients for  $E=0.6$  ( $.58 < r/D < 1.00$ )
12. Comparison of Model Results with Experimental Pressure  
Contours for  $E=0.6$
13. Comparison of Model Results with Experimental Pressure  
Coefficients with Application of Wake Region Considerations  
( $E=0.6$ ,  $0^\circ < \theta < 90^\circ$ )

14. Comparison of Model Results with Experimental Pressure  
Coefficients with Application of Wake Region Considerations  
( $E=0.6$ ,  $105^\circ \leq \theta < 180^\circ$ )
15. Comparison of Model Results with Experimental Pressure  
Coefficients with Application of Wake Region Considerations  
( $E=0.6$ ,  $.58 < r/D < 1.00$ )
16. Comparison of Model Results with Experimental Pressure  
Contours with Application of Wake Region Considerations  
( $E=0.6$ )
17. Comparison of Model Results with Results of Thompson (ref. 4)
18. Comparison of Model Results with Results of Bradbury and  
Wood (ref. 5)
19. Comparison of Model Results and Experimental Lift and Moment  
on the Flat Plate
20. Comparison of Model Results and Experimental Pressure  
Coefficients (Vortices Begin at Edges of Jet Orifice)

# SYMBOLS

$a, b, c$	constants defined by equation (11)
$A$	constant defined by equation (7)
$B$	constant defined by equation (8)
$C, C'$	constants defined by equations (9) and (10)
$C_p$	pressure coefficient
$D$	jet orifice diameter, m (ft)
$E_e$	entrainment coefficient for zone of flow establishment
$E$	entrainment coefficient for zone of established flow
$e_{\theta_1}, e_{\theta_2}, e_{\theta_3}$	unit vectors defined by Figure 2
$h$	effective vortex half spacing, m (ft)
$h_o$	diffuse vortex half spacing, m (ft)
$K_1, K_2, K_3, K_4$	constants defined by equations (18) and (19)
$L$	lift on flat plate, N (lbf)
$M$	moment on flat plate, N-m (lbf-ft)
$Q$	jet volume flux, $m^3/sec$ ( $ft^3/sec$ )
$Q_o$	jet volume flux at jet orifice, $m^3/sec$ ( $ft^3/sec$ )
$q$	sink strength density, $m^2/sec$ ( $ft^2/sec$ )
$r$	polar coordinate, m (ft)
$R$	jet to crossflow velocity ratio, $U_j/U_\infty$
$S$	arc distance along jet centerline or vortex curve, m (ft)
$S_c$	critical arc length, m (ft)
$T$	jet thrust, N (lbf)

$U$	fluid speed on flat plate, m/sec (ft/sec)
$U_j$	jet velocity, m/sec (ft/sec)
$U_\infty$	free stream velocity, m/sec (ft/sec)
$X, Y, Z$	axes in tunnel coordinate system, m (ft)
$\beta$	vortex diffusivity, $m^{-1}$ ( $ft^{-1}$ )
$\Gamma$	effective vortex strength, $m^2/sec$ ( $ft^2/sec$ )
$\Gamma_0$	integrated strength of a single diffuse vortex, $m^2/sec$ ( $ft^2/sec$ )
$\gamma_0$	dimensionless variable corresponding to $\Gamma_0$
$\omega$	vorticity, $sec^{-1}$
$\omega_0$	maximum vorticity in cross section, $sec^{-1}$
$\theta$	polar coordinate, degrees

Abstract of Thesis Presented to the Graduate Council  
of the University of Florida in Partial Fulfillment of the Requirements  
for the Degree of Master of Science

A METHOD FOR CALCULATING THE  
INDUCED PRESSURE DISTRIBUTION ASSOCIATED  
WITH A JET IN A CROSSFLOW

By

William E. Dietz, Jr.

December, 1975

Chairman: Richard L. Fearn  
Major Department: Engineering Sciences

A model is formulated to predict numerically the pressure distribution induced by a round, turbulent, unheated, subsonic jet exhausting normally through a flat plate into a subsonic crossflow. The complete model assumes that the predominant features of the flow are jet entrainment and a pair of contra-rotating vortices which form downstream of the jet. Experimentally determined vortex properties and a reasonable assumption concerning jet entrainment are used. Potential flow considerations are used except in the wake region, where a simple method for approximating the pressure distribution is suggested. The calculated pressure distribution, lift, and pitching moments on the flat plate are presented for a jet to crossflow velocity ratio of 8 and are compared with experimental results.

  
Chairman



## INTRODUCTION

During the transition from hovering to horizontal flight, a VTOL aircraft may experience loss of lift and undesirable pitching moments due to the effects of one or more jets exhausting normally into the crossflow created by the craft's forward motion. Figure 1 is a sketch which gives a qualitative description of the flow field resulting from a single-jet VTOL aircraft transitioning from hovering to horizontal flight. The interaction of the jet and crossflow induces a pressure distribution on the lower surfaces of the craft, resulting in loss of lift and, in most cases, a nose-up pitching moment. Although most VTOL craft employ multiple jets which are of a higher temperature than the surrounding air, it is generally desirable to simplify the problem to a case which lends itself to experimental and theoretical analysis while still retaining the basic characteristics of the jet and crossflow interaction process. Therefore, it is convenient to restrict the problem to that of a single, unheated, subsonic jet exhausting at large angles through a flat plate into a subsonic crossflow. This simplified case has applications in problems other than the transitioning of VTOL craft, such as the problem of cooling gases in turbine combustors and the discharge of effluent or cooling water into a waterway.

Early investigations into the problem of a jet in a crossflow were concerned with studies of the jet deflection resulting

from the interaction of the jet and crossflow. These studies resulted in empirical relationships for the jet centerline which is defined as the locus of points of maximum velocity in the symmetry plane (ref. 1). Recent investigations into the velocity field associated with a jet in a crossflow have shown the jet wake region to be dominated by a pair of contrarotating vortices which form downstream of the jet and to either side of the symmetry plane. Fearn and Weston (ref. 2) investigated the case of an unheated jet exhausting normally into a crossflow and formulated empirical relationships for the characteristics of the vortex pair.

The pressure distribution on the flat plate has received considerable attention by several investigators. Fearn and Weston (ref. 3), Thompson (ref. 4), and Bradbury and Wood (ref. 5) investigated the flat plate pressure distribution for several jet to crossflow velocity ratios. Wooler (ref. 6) and Thompson each attempted to predict numerically the flat plate pressure distribution by modelling the various features of the flow with potential flow singularities. The development of potential flow models was limited by the lack of data concerning the characteristics of the vortex pair. Also, the use of potential flow modelling alone resulted in erroneous pressure calculations in the wake region downstream of the jet.

This paper will present a method for calculating the flat plate pressure distribution associated with a jet in a crossflow. As in the models presented by Thompson and by Wooler, potential

flow singularities are incorporated. However, in this study, the model incorporates the physical characteristics of the vortex pair, as described by Fearn and Weston (ref. 2) and extended by Sellers (ref. 7). As a result, the model is more consistent with the flow field actually observed than were the previous modelling attempts. In addition, a means of approximating the pressure distribution in the wake region is suggested. Therefore, a fairly complete description of the flat plate pressure distribution, based on the physical characteristics of a jet in a crossflow, may be accomplished. The model is applicable for all velocity ratios, as long as a graphical or analytic description of the vortex properties is available. For this study, it is desired to demonstrate the applicability of this model when used in conjunction with an analytic description of the vortex pair. Since an adequate analytic description of the vortex properties is available only for a jet to crossflow velocity ratio of 8 (ref. 7), the model presented in this thesis is restricted to this case.

## LITERATURE REVIEW

In order to fully appreciate the problems encountered in the analysis of the jet in a crossflow, it is necessary to review briefly some past attempts at modelling the flow and predicting the flat plate pressure distribution. Generally, attempts to predict the pressure distribution on the flat plate have been limited in success, due to the lack of data concerning entrainment by the jet and the nature of the vortex pair.

Numerical predictions of the flat plate pressure distribution generally rely on the use of potential flow singularities to model the jet and vortex pair. The pressure field is related to the numerically calculated potential or velocity field through Bernoulli's equation. Generally, no account can be made for the wake region through the use of potential flow modelling alone, since energy losses through viscous effects and separation result in the inapplicability of a potential flow solution.

Thompson (ref. 4) attempted to predict the flat plate pressure distribution by modelling the jet and vortices with a distribution of sinks and doublets placed along the jet centerline. Since the vortex spacing is generally small compared to the distance to a typical field point, Thompson assumed that the vortex pair could be modelled as a distribution of finite horseshoe vortices distributed along the jet centerline. Since such a system of vortices is equivalent to a distribution of axially normal source-sink doublets (ref. 4 and ref. 8, pg. 96), Thompson placed a distribution of

doublets along the jet centerline. To account for mass entrainment by the jet, a distribution of line sinks was also placed along the jet centerline. Although Thompson recognized that the vortex trajectories lie to either side of the symmetry plane and that their projection onto the symmetry plane does not coincide with the jet centerline, the doublets were placed along the jet centerline for analytical convenience. The doublet strengths were obtained through experimental measurements of the velocity field, while the strength of the sink distribution was assumed constant and its value determined by matching experimental and predicted upstream pressure contours. Thompson analyzed several cases, for velocity ratios of 2, 4, and 8, both with and without the sink distribution. The pressure distribution was accounted for fairly well by the model incorporating both the sink and doublet distribution. The model incorporating only the doublet distribution could not account for the pressure distribution upstream of the jet orifice. As expected, both models failed in the wake region.

Wooler (ref. 6) attempted a numerical analysis of the flat plate pressure distribution using two different potential flow models. The first, which Wooler called the vorticity model, idealized the jet as a system of horseshoe vortices placed along the jet centerline. The strength of each vortex was determined from the jet momentum flux and the radius of curvature of the jet centerline. A contour plot of the pressure distribution on the flat plate shows good agreement with the experimental results of Bradbury and Wood (ref. 5) except for the wake region and the area upstream of the

jet orifice.

Wooler's second method, called the sink-doublet model, utilized a system of sinks and doublets distributed along the jet centerline. The doublets institute a blockage of the free stream by the jet, essentially modelling the jet as a cylinder of elliptic cross section. The sink distribution along the jet centerline models entrainment of the surrounding air by the jet. The sink strengths were determined by solving equations for the jet development such that they provide a best fit with experimental test data. The doublet strengths were obtained from the complex velocity potential for two-dimensional flow past an ellipse. Wooler did not attempt to calculate the pressure contours on a flat plate using this model, but instead calculated wing loadings caused by a jet issuing from the center of a wing. The numerical results for particular spanwise and chordwise data points correlate well with Wooler's experimental data. However, the choice of data points did not include the wake region or the region upstream of the jet.

In the models presented by Wooler and by Thompson, singularities modelling the vortex pair were placed along the jet centerline rather than along the true vortex trajectories. In addition, vortex strengths were, in the case of Wooler's model, obtained from assumptions concerning growth of the jet plume rather than from an experimental description of the vortex pair.

A recent experimental study by Fearn and Weston (ref. 2) has provided a quantitative description of the vorticity associated with a jet in a crossflow. This information was found to be

useful in the formulation of a more realistic model for calculating the pressure distribution on the flat plate. The authors presented two models for the vortex pair. The first, known as the filament model, idealized the vortex pair as two filament vortices. It was assumed that the characteristics of the vortex pair change slowly along the vortex curve. Hence, the velocity field at a cross section perpendicular to the vortex curve was assumed to be equivalent to that produced by two infinite filament vortices perpendicular to the cross sectional plane. From experimentally determined velocities in the symmetry plane, the strength and spacing of the filament vortices at the cross section were obtained. The second model, known as the diffuse model, relaxed the assumption of concentrated vorticity and assumed the vorticity distribution of each vortex to be Gaussian in nature. Figure 2 shows the coordinate system used in the description of the diffuse model. The vorticity at any point was assumed to be

$$\omega(r, \theta) = \omega_0 (e^{-\beta^2 r_1^2} - e^{-\beta^2 r_2^2}) \quad (1)$$

where  $\omega_0$  is the maximum vorticity in the cross section, and  $\beta$  is the diffusivity of the vortices. The integrated strength  $\Gamma_0$  of a single diffuse vortex was defined as

$$\Gamma_0 = \int_0^{2\pi} \int_0^\infty \omega_0 e^{-\beta^2 r^2} r dr d\theta \quad (2)$$

The net effective strength  $\Gamma$  of each diffuse vortex was defined as the net flux of vorticity across the half plane of the cross

section

$$\Gamma = \int_{-\pi/2}^{\pi/2} \int_0^{\infty} \omega(r, \theta) r dr d\theta \quad (3)$$

The effective spacing  $h$  was defined to be the center of vorticity

$$h = \frac{1}{\Gamma} \int_{-\pi/2}^{\pi/2} \int_0^{\infty} \omega(r, \theta) Y_v r dr d\theta \quad (4)$$

Equations (3) and (4) were evaluated using the assumed distribution of vorticity to give

$$\Gamma = \Gamma_0 \operatorname{erf}(\beta h_0) \quad (5)$$

and

$$h = h_0 / \operatorname{erf}(\beta h_0) \quad (6)$$

where

$$\operatorname{erf}(\beta h_0) = \frac{2}{\sqrt{\pi}} \int_0^{\beta h_0} e^{-t^2} dt$$

is the error function. The authors found that the parameters of both vortex models were functions primarily of the jet to crossflow velocity ratio,  $R$ , and of arc distance along the vortex curve,  $S/D$ . The results of this investigation were presented graphically. It was observed that the vortex strength  $\Gamma_0$  determined from the diffuse vortex model was not a function of  $S/D$  and could be written as a linear function of  $R$ . The expression for the integrated strength  $\Gamma_0$  was written

$$\Gamma_0 = AR \quad (7)$$



where  $A$  is a constant equal to 0.72 and  $\gamma_0$  is the integrated strength,  $\Gamma_0$ , non-dimensionalized by  $2DU_\infty$  for convenience. The quantity  $2DU_\infty$  was found by Chang-Lu (ref. 9) to be equal to the roll up of the vorticity around a two dimensional cylinder.

Equations (5), (6), and (7) represent a description of the strength and spacing of the vortex pair, but contain two parameters,  $\beta$  and  $h_0$ , which must be specified for the description to be complete.

In this study, it is desired to demonstrate the use of the model in conjunction with analytic descriptions of the vortex pair, even though the model may be used with either graphical or analytic descriptions of the vortices. At this time, analytic relationships for  $\beta$  and  $h_0$  have been developed only for a velocity ratio of 8.

Sellers (ref. 7), in an extension of the work by Fearn and Weston, formulated relationships for  $\beta$  and  $h_0$  as functions of  $S/D$  and  $R=8$ .

The equations may be written

$$\beta D = \frac{B}{(S/D)^{1/2}} \quad (8)$$

and

$$\frac{h_0}{D} = C \left( 1 - e^{-\frac{S/D}{8}} \right) \quad (9)$$

where  $B=2.11$  and  $C=2.04$ . With these analytic descriptions for  $\beta$  and  $h_0$ , the effective strength  $\Gamma$  and spacing  $h$  of the vortex pair for a velocity ratio of 8 may be calculated as a function of  $S/D$ .

Equations (8) and (9) are based on the assumption that the vortices begin at the center of the jet orifice. Since most of

the velocity field data was taken at  $S/D > 5$ , there is considerable doubt as to the nature of the vortex trajectories close to the jet orifice. Sellers also presented an equation for  $h_o$  which would result in the vortices intersecting the flat plate at the edges of the jet orifice. The equation, again valid only for  $R=8$ , may be written

$$\frac{h_o}{D} = C' \left( 1 - e^{\frac{-s/D}{8}} \right) + .5 \quad (10)$$

where  $C'=1.389$  .

Fearn and Weston (ref. 2) also formulated relationships for the jet centerline and vortex curve. An equation of the form

$$Z/D = a R^{b_c} (X/D)^{c_c} \quad (11)$$

describes the jet centerline and the vortex curve adequately. For the jet centerline,  $a_c=0.9772$ ,  $b_c=0.9113$ , and  $c_c=0.3346$  . For the vortex curve,  $a_v=0.3473$ ,  $b_v=1.127$ , and  $c_v=0.4291$  .

The equations formulated by Fearn, Weston, and Sellers give a fairly complete analytic description of the vortex pair for  $R=8$ , providing a basis for the formulation of a realistic model for calculating the flat plate pressure distribution induced by a jet in a crossflow.

# FORMULATION OF THE PROBLEM

The relationships for the characteristics of the vortex pair introduced by Fearn and Weston (ref. 2) and extended by Sellers (ref. 7) make possible the formulation of a model for the vortex pair which may be used in a numerical analysis conducted through the use of a digital computer. The relationships are repeated for convenience.

$$\Gamma = \Gamma_0 \operatorname{erf}(\beta h_0) \quad (5)$$

$$h = h_0 / \operatorname{erf}(\beta h_0) \quad (6)$$

$$\Gamma_0 = 2DU_\infty AR = 2ADU_j \quad (7)$$

$$Z/D = aR^b(X/D)^c \quad (11)$$

$$\beta D = \frac{B}{(S/D)^{1/2}} \quad (8)$$

$$\frac{h_0}{D} = C \left( 1 - e^{-\frac{S/D}{8}} \right) \quad (9)$$

Equations (5), (6), (7), and (11) are general in that they are valid for all  $S/D$  and  $R$  within the range of the experiment, that is, for  $5 < S/D < 45$  and  $2 < R < 10$ . Equations (8) and (9) are, as pointed out earlier, valid only for  $R=8$ .

The vortices are modelled in the computer program by a distribution of finite filament vortices placed along the vortex trajectories described by equations (6) and (11). The strengths of the finite filaments are given by equation (5). Although it is well established that the vortices are diffuse in the actual case of a

jet in a crossflow, it is assumed that the velocity induced at a field point by a filament vortex will be indistinguishable from the velocity induced by a diffuse vortex, as long as the distance from the filament is large compared to the radius of the diffuse core. Since the diffuse vortices are observed to vary in strength along the vortex curve as a result of diffusion of vorticity across the symmetry plane, the strengths of the filament vortices are varied as a function of  $S/D$  in the computer model. Although this is inconsistent with Helmholtz's Laws, it should be emphasized that the filament vortices are used for analytical convenience and are modelling a diffuse vortex pair, for which there are no restrictions regarding the variation in strength along the vortex trajectories.

The distribution of filament vortices is composed of finite straight line segments, the lengths of which are determined by the local radius of curvature of the vortex curve. Enough vortex segments are generated such that the addition of more segments results in negligible velocity changes at the plane of the flat plate.

A distribution of line sinks is placed along the experimentally determined jet centerline, defined by equation (11). Although little data is available concerning entrainment by a jet in a crossflow, experimental and theoretical analyses are available for a free jet which may provide a basis for estimating the amount of entrainment by a deflected jet and thereby establishing the strengths of the line sinks.

A free jet is usually described in terms of two regions, each characterized by different cross sectional velocity profiles (ref. 10). The first region, known as the zone of establishment, begins at the jet orifice and may be idealized as a jet core, characterized by a flat velocity profile, surrounded by a turbulent fluid. The core is roughly conical in shape, and diminishes in cross sectional area along the jet centerline as a result of shear produced by the differing mean velocities of the jet and the surrounding fluid. When the core disappears (at some  $S/D$  defined as the critical length), the flow is said to be fully established, and is characterized by a velocity profile roughly Gaussian in nature.

Albertson (ref. 10) conducted a theoretical analysis of a free jet and formulated relationships for the entrainment in the zone of establishment and in the region of established flow. Albertson found that the ratio of cross sectional jet volume flux to volume flux at the jet orifice increased in a parabolic form

$$\frac{Q}{Q_0} = 1 + 0.083\left(\frac{S}{D}\right) + 0.0128\left(\frac{S}{D}\right)^2 \quad (12)$$

in the zone of establishment. In the zone of established flow, the relationship is linear

$$\frac{Q}{Q_0} = 0.32\left(\frac{S}{D}\right) \quad (13)$$

It is convenient to express the amount of entrainment in terms of

an entrainment coefficient  $E$

$$E = \frac{1}{Q_0} \frac{dQ}{d(s/D)} \quad (14)$$

Using Albertson's relationships, the entrainment coefficient may be expressed

$$E_e = 0.083 + 0.0256 \left( \frac{s}{D} \right) \quad (15)$$

in the zone of establishment, and

$$E = 0.32 \quad (16)$$

for established flow. The constant entrainment coefficient of 0.32 for a fully developed jet has been confirmed by Ricou and Spaulding (ref. 11) and Saha (ref. 15).

A free jet entrains surrounding fluid primarily through turbulent shear resulting from the difference in velocity of the jet and the surrounding fluid. The entrainment mechanism is considerably more complex in the case of a jet in a crossflow. Keffer (ref. 14) states that a jet in a crossflow entrains surrounding fluid not only through turbulent shear, but also through the effects of free stream and vortex upwash components perpendicular to the jet trajectory. In addition, increased shear at the boundary of the jet resulting from the presence of the crossflow results in a more rapid degradation of the jet core and a decrease in the critical length.

Because of the lack of experimental data concerning entrainment by a jet in a crossflow, it is necessary to attempt to qualitatively

estimate the entrainment coefficient  $E$  for use in the computer model. It is logical to assume that the entrainment coefficient  $E$  will be larger than 0.32, the value for a free jet. It is assumed that  $E$  is constant for a fully established deflected jet, based on observations of free jets. An upper limit for the entrainment coefficient has been suggested by Fearn (ref. 13) in an attempt to account for the observed jet trajectory entirely on the basis of mass entrainment by the jet. For a velocity ratio of 8, an entrainment coefficient of approximately 1.2 was calculated for the region of established flow. Therefore, the value of  $E$  used in the model would be expected to have a value between 0.32 and 1.2 .

The strength density of the line sinks is expressed in terms of the change in jet volume per unit length  $S/D$ , or

$$q = \frac{dQ}{d(s/D)} \quad (17)$$

Relations for  $q$  for a jet in a crossflow were found by assuming

$$\frac{Q}{Q_0} = K_1 + K_2 \left( \frac{s}{D} \right) + K_3 \left( \frac{s}{D} \right)^2 \quad (18)$$

for the zone of establishment, and

$$\frac{Q}{Q_0} = K_4 \left( \frac{s}{D} \right) \quad (19)$$

for established flow. These relations are of the same form as Albertson's equations for free jets. By definition

$$E = \frac{1}{Q_0} \frac{dQ}{d(s/D)} = K_4 \quad (20)$$

The coefficients  $K_1$ ,  $K_2$ , and  $K_3$  are found by applying boundary conditions. It is assumed that  $Q=Q_0$  at  $S/D=0$ ,  $\frac{1}{Q_0} \frac{dQ}{d(S/D)} = 0$  at  $S/D=0$ , and  $\frac{1}{Q_0} \frac{dQ}{d(S/D)}$  is continuous at the critical length. Equations (18) and (19) then become

$$\frac{Q}{Q_0} = 1 + \frac{1}{2} \frac{E}{(S_c/D)} (S/D)^2 \quad (21)$$

for the zone of establishment, and

$$\frac{Q}{Q_0} = E \frac{S}{D} \quad (22)$$

for established flow. From these relationships, the strength density  $q$  may be written

$$q = \frac{E Q_0 (S/D)}{(S_c/D)} \quad (23)$$

in the zone of establishment, and

$$q = \frac{E Q_0}{D} \quad (24)$$

for established flow. The amount of entrainment is therefore defined by establishing values for  $E$  and  $S_c/D$ . From Keffer (ref. 14) and Fearn (ref. 13), the critical length  $S_c/D$  is equal to about 3 for a velocity ratio of 8. This value, although approximate, has more experimental basis than values of  $E$  for deflected jets.

Therefore,  $E$  was the only parameter which was varied in the model. The value for  $E$  was adjusted until the model provided good overall correlation with the experimentally determined pressure distribution.

With the preceding description of the vortices and sinks incorporated into the model, it was possible to calculate the



velocity induced on the flat plate. This is accomplished through vector summation of the velocities induced on the flat plate by each incremental vortex and sink filament. "Image" vortex and sink distributions are instituted "below" the flat plate in order to establish the boundary condition at the plane of the flat plate, as shown in Figure 3. With the velocity field on the flat plate determined, the pressure coefficients at each field point may be calculated from Bernoulli's equation. The pressure coefficient is derived from Bernoulli's equation and may be written

$$C_p = 1 - \frac{U^2}{U_\infty^2} \quad (25)$$

where  $U$  is the fluid speed at a particular field point.

The pressure distribution on the flat plate is most conveniently presented by defining the field points in terms of polar coordinates. Figure 4 shows the tunnel and field point coordinate systems used in the experimental investigations of Fearn and Weston (ref. 3). Each field point is expressed in terms of  $r/D$  and  $\theta$ . Fearn and Weston presented pressure coefficient data in terms of contour plots and pressure distribution along rays (constant angle  $\theta$ ) and circles (constant  $r/D$ ). The results of Fearn and Weston are used for comparison with the theoretical results of the model in Figures 5 through 16.

As expected, the pressure coefficients predicted by the model were found to be in considerable error in the wake region, due to viscous effects and separation. For the purposes of this study, a wake boundary is defined by comparing contour plots of

experimental and theoretical pressure distributions and fitting a power curve through the points where the theoretical results begin to deviate significantly from the experimental contours. This wake boundary, which is defined for the purposes of this study only, should not be confused with that which would be observed through oil smear studies or other flow visualization techniques. It is assumed that a point on the wake boundary defines the pressure at all points in the wake region with the same X-coordinates as the point on the boundary. The elimination of Y-dependent pressures results in straight contour levels extending from the wake boundary to the X-axis. From studying contour plots of the experimental pressure distribution for various velocity ratios (ref. 3), it appears that this method for approximating the pressures in the wake region should be applicable for velocity ratios greater than 5. At lower velocity ratios, the contours in the wake region cannot be approximated by straight lines, due to the tendency for the contours to become increasingly curvilinear at lower velocity ratios.

Lift and pitching moments on the flat plate are calculated for the complete model. Lift is calculated by summing forces on incremental areas of the flat plate. Moment about the Y-axis is found by multiplying incremental areas by the distance from the Y-axis, and summing over a large area of the flat plate.

## RESULTS

The simplest form of the model consists of the vortex distribution alone, with the vortices intersecting the flat plate at the center of the jet orifice. In this simplified form, it is assumed that the flat plate pressure distribution results from the vortex pair and free stream interaction only. Figures 5 through 8 compare the experimental pressure coefficients with the theoretical values predicted for this case. Figures 5 and 6 show the variation of the pressure coefficient with radial distance from the center of the jet orifice for given values of  $\theta$ . The plots show fairly good agreement with experiment from about  $\theta=75^\circ$  to  $\theta=120^\circ$ . From  $120^\circ$  to  $180^\circ$  the theoretical values deviate considerably from the experimental results, as expected, since conditions in the wake region render potential flow considerations invalid. The theoretical values from  $\theta=0^\circ$  to  $\theta=75^\circ$  also deviate significantly from the experimental values, due to the neglect of jet flow entrainment, as will be shown later. Figure 8 shows a contour plot of the pressure distribution induced by the vortices alone. The theoretical contours clearly deviate greatly from experimental values outside the  $\theta=75^\circ$  to  $\theta=120^\circ$  range.

Figures 9 through 12 show the effects of adding a sink distribution along the jet centerline to account for entrainment effects. In this study, good results were obtained for  $E=0.6$ , with a critical length of 3 jet diameters. The value of the entrainment coefficient is within the range expected, i.e.  $0.32 < E < 1.2$ .

It is evident that the addition of a sink distribution greatly improves the accuracy of the model in regions upstream of the jet orifice. The greatest errors outside the wake region occur at low  $r/D$  ( $<1.0$ ) during the transition from positive to negative pressure coefficients in the range  $\theta=20^\circ$  to  $\theta=45^\circ$ , as can be seen in Figure 9. However, Figure 12 shows that the theoretical and experimental contours are quite close in this region. It may also be seen that the density of contours in this region indicate that high pressure gradients exist. Hence, a small displacement of the contours results in a large change in pressure values displayed in the radial plots, suggesting that the rather large errors observed in the radial plots for this region are a result of the manner in which the data is presented, rather than a result of a serious failure of the model. Good agreement is obtained up to about  $\theta=135^\circ$ , at which point viscous effects and separation appear to become important. The largest error observed on the contour plot (Figure 12) is on the order of one jet diameter, and involves the  $-0.2$  contour at about  $45^\circ$ . This is not considered to be a particularly significant error, since insignificant variations in pressure can cause noticeable shifts in the placement of contours in regions of very small pressure gradients.

The potential flow model results in pressure coefficients being too large in the wake region. As stated earlier, the failure of the model in the wake region is not unexpected. However, a complete description of the pressure distribution must take the wake region into account in some manner. Figures 13 through 16

show the resulting pressure field for a model incorporating both jet entrainment and wake region considerations described in the previous section. It may be seen that the accuracy of the theoretical wake region pressures is greatly improved, although good quantitative agreement has not been achieved for  $r/D$  of less than 1.5. Figure 16 shows the contour plot for the complete model. From the contour plot, it may be seen that the largest discrepancies occur in the wake region for  $C_p = -0.1$ . This is not considered to be significant, since this region is characterized by very low pressure gradients and a large uncertainty in contour placement. Figures 17 and 18 show the theoretical results of the complete model compared with the experimental results of Thompson (ref. 4) and Bradbury and Wood (ref. 5). It may be seen that the contours agree quite well with Thompson's results. Agreement with the results of Bradbury and Wood is not as close, but is still considered to be within the range of experimental error.

The lift and pitching moments on the flat plate are of special interest, particularly in the case of transitioning VTOL craft. Figure 19 shows a plot of experimental values of  $M/TD$  and  $L/T$  versus the velocity ratio  $R$ . The circles represent values of  $M/TD$  and  $L/T$  predicted by the complete model for a velocity ratio of 8. The theoretical values show good agreement with the experimental values.

Sellers (ref. 7) formulated a model in which the vortices intersect the flat plate at the edges of the jet orifice, rather than at the center. Although this model may seem more physically

reasonable, the resulting pressure distribution predicted by the model (Figure 20) deviates considerably from the experimental data. The extremely low pressure coefficients result from a combination of the effects of non-zero vortex strength at the plane of the flat plate and the proximity of the filament vortices to the field points closest to the jet orifice. It is evident that a model based on vortices beginning at the edges of the jet orifice is incompatible with the use of filament vortices.

## CONCLUSION

The pressure distribution calculated from the model presented in this thesis is in fairly good agreement with experimental data. The use of this model was demonstrated for a velocity ratio of 8 in order to make use of an available analytic description of the characteristics of the vortex pair. The model is equally applicable for other velocity ratios when used in conjunction with graphical descriptions of the vortex properties. The method for predicting wake region pressures is expected to be applicable for velocity ratios greater than 5; at lower velocity ratios, curved lines may be necessary to approximate the shape of the wake contours.

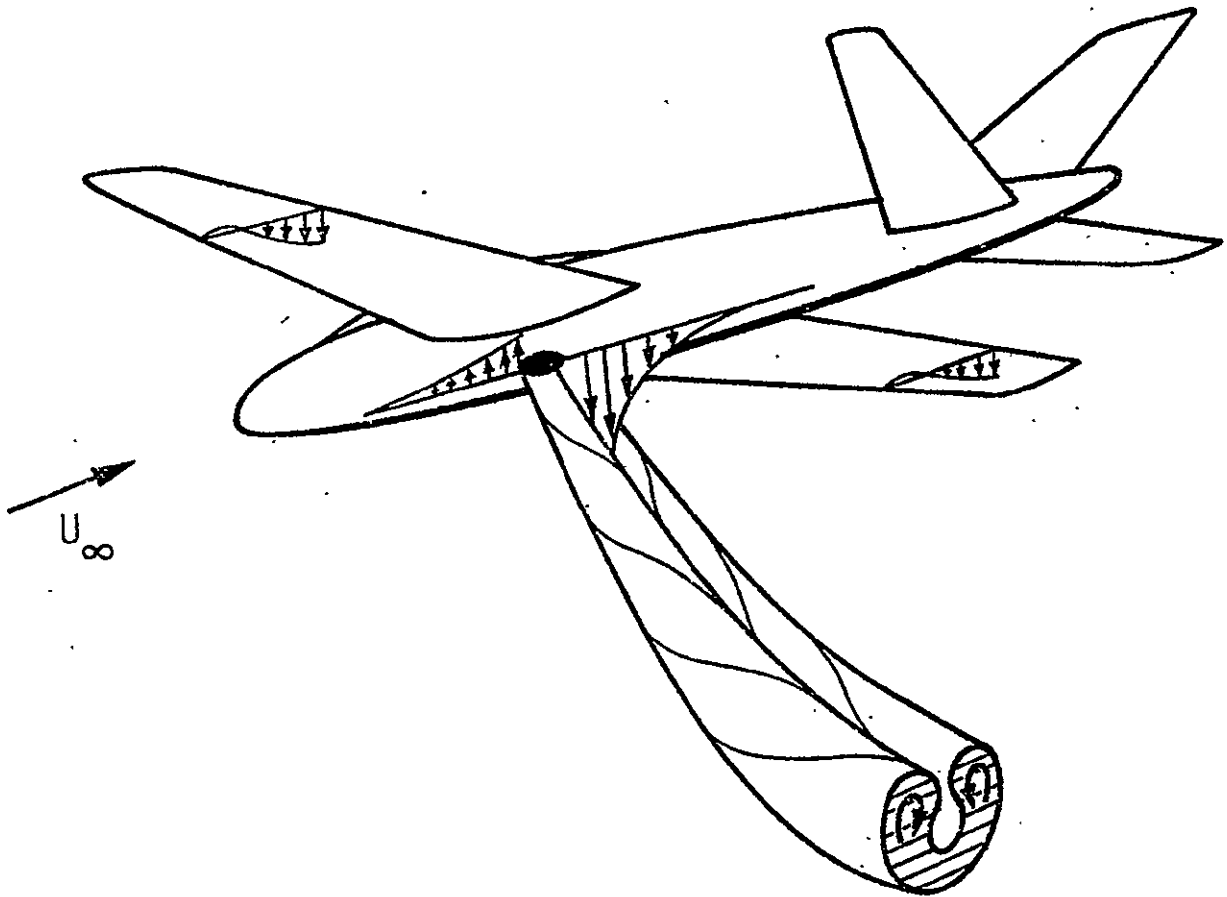


Figure 1. Sketch of VTOL Aircraft Transitioning  
from Hovering to Horizontal Flight





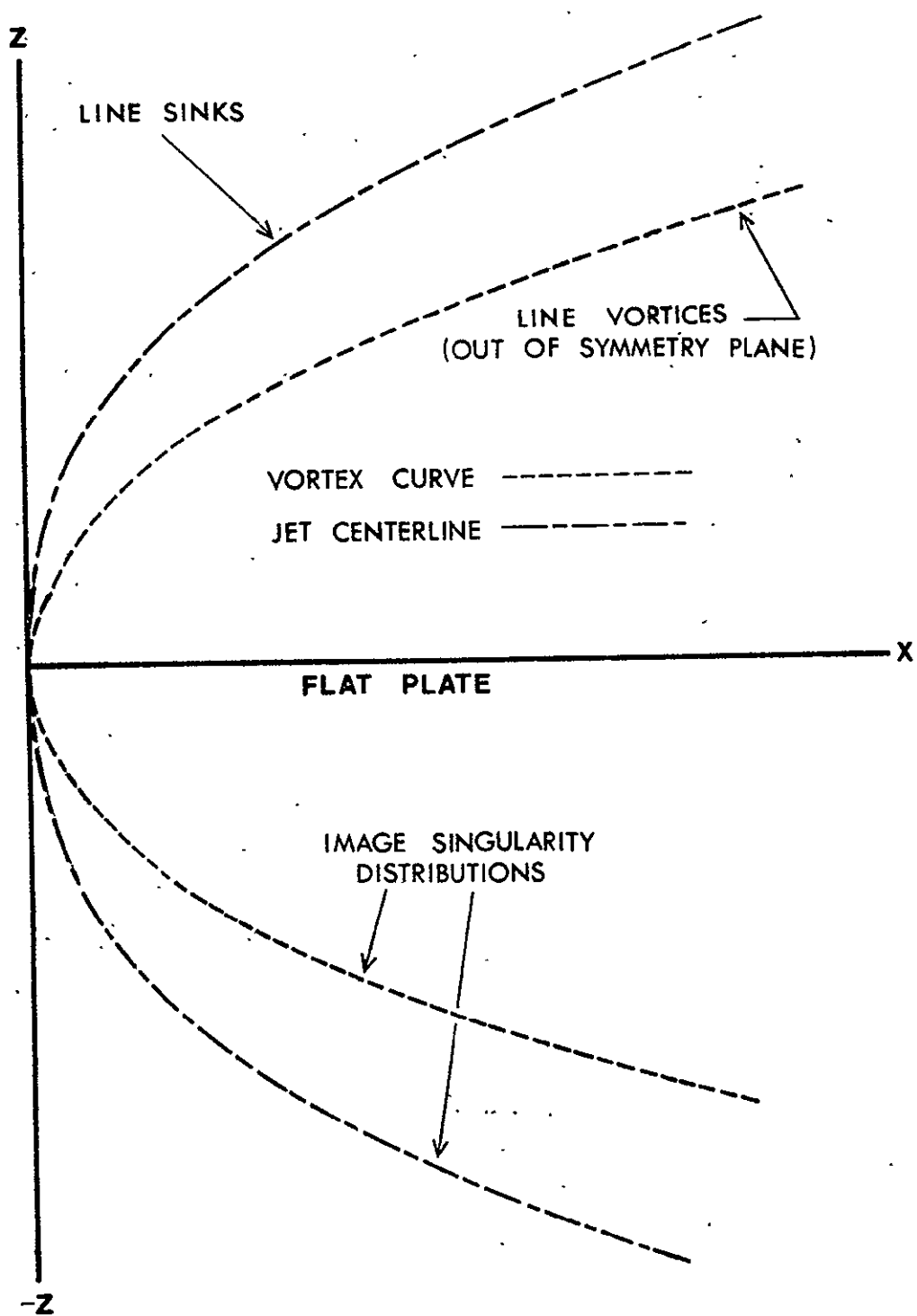


Figure 3. Arrangement of Singularity Distributions in the Model

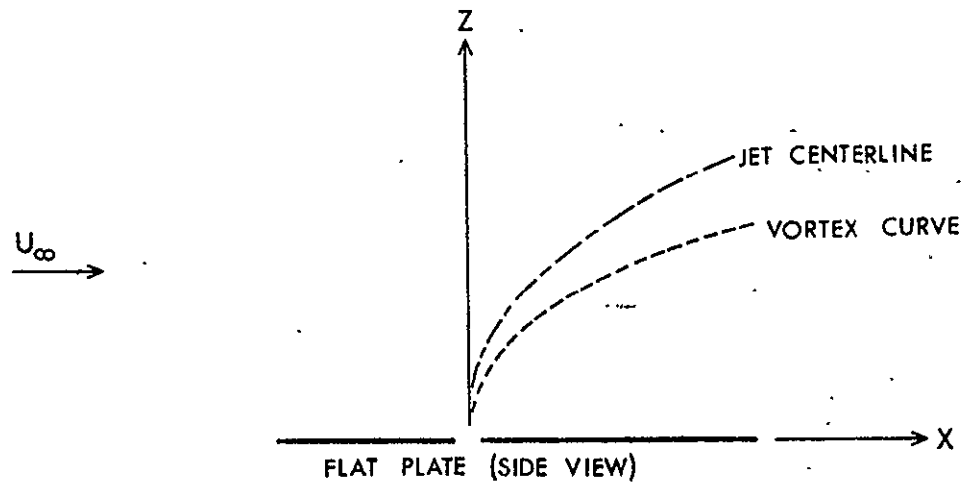
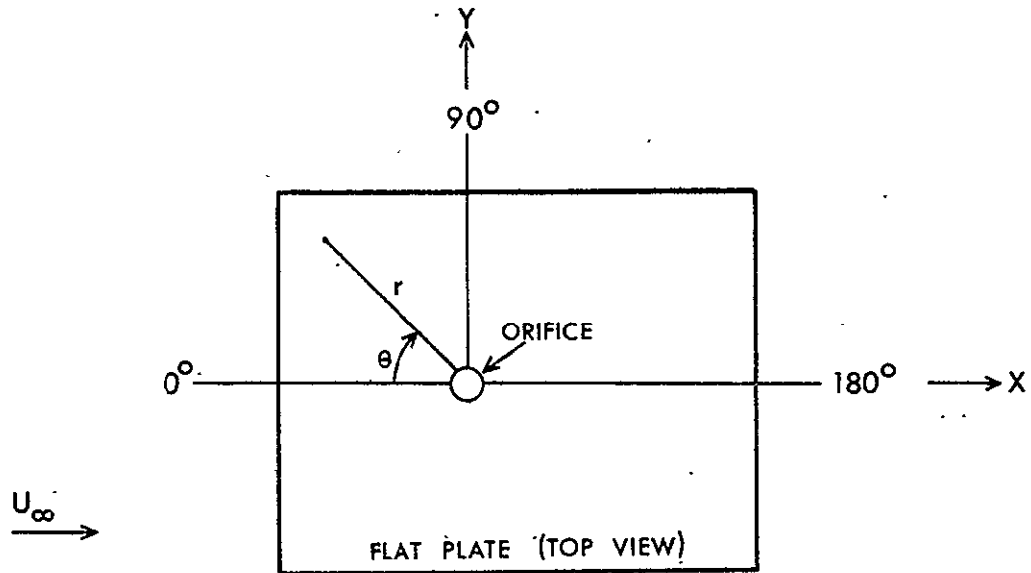


Figure 4. Tunnel and Field Point Coordinate Systems

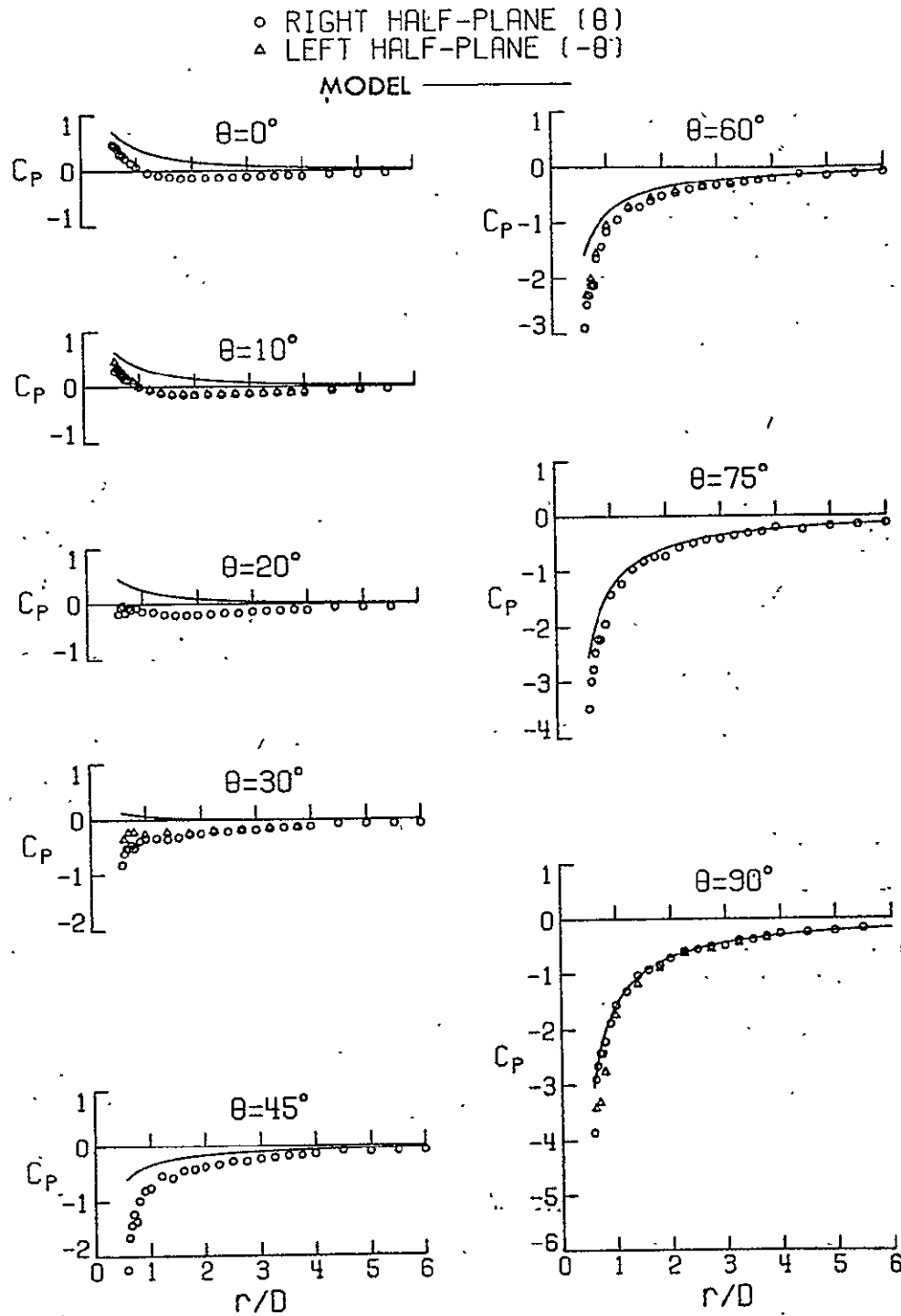


Figure 5. Comparison of Model Results with Experimental Pressure Coefficients for Zero Entrainment ( $0^\circ < \theta < 90^\circ$ )

REPRODUCIBILITY OF THE  
 ORIGINAL PAGE IS POOR

○ RIGHT HALF-PLANE ( $\theta$ )  
 ▲ LEFT HALF-PLANE ( $-\theta$ )  
 MODEL ———

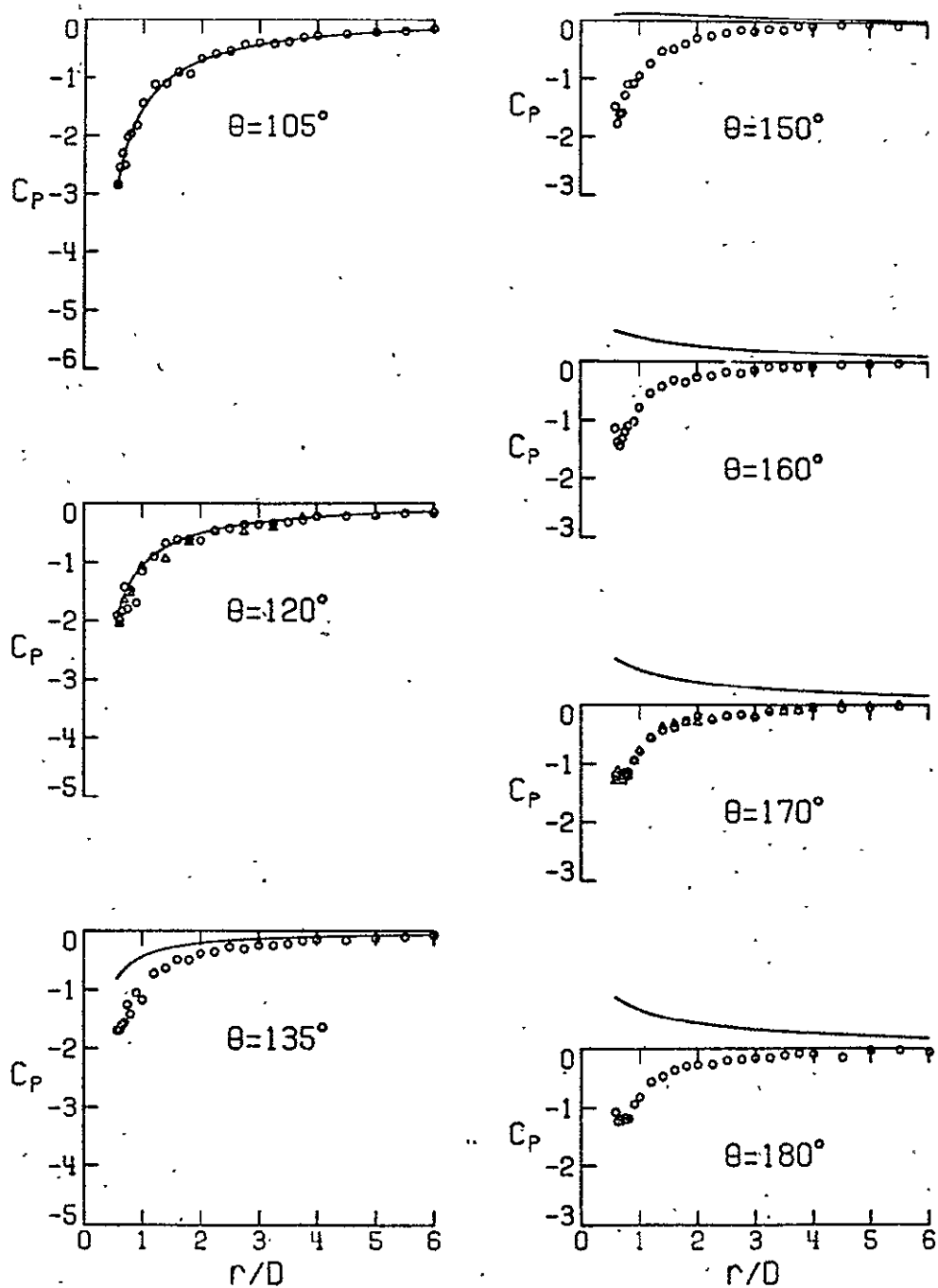


Figure 6. Comparison of Model Results with Experimental Pressure Coefficients for Zero Entrainment ( $105^\circ < \theta < 180^\circ$ )

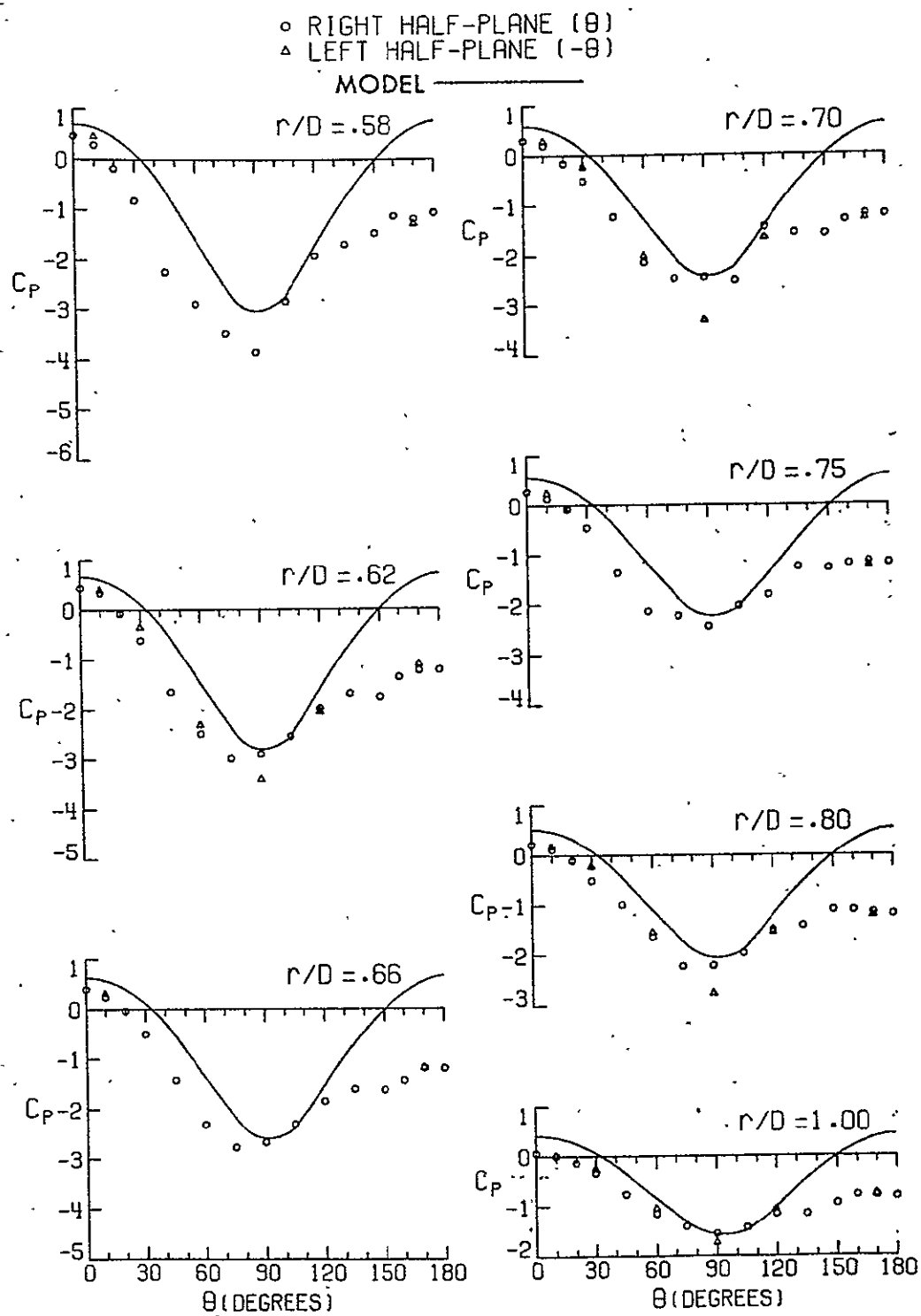


Figure 7. Comparison of Model Results with Experimental Pressure Coefficients for Zero Entrainment ( $.58 < r/D \leq 1.00$ )

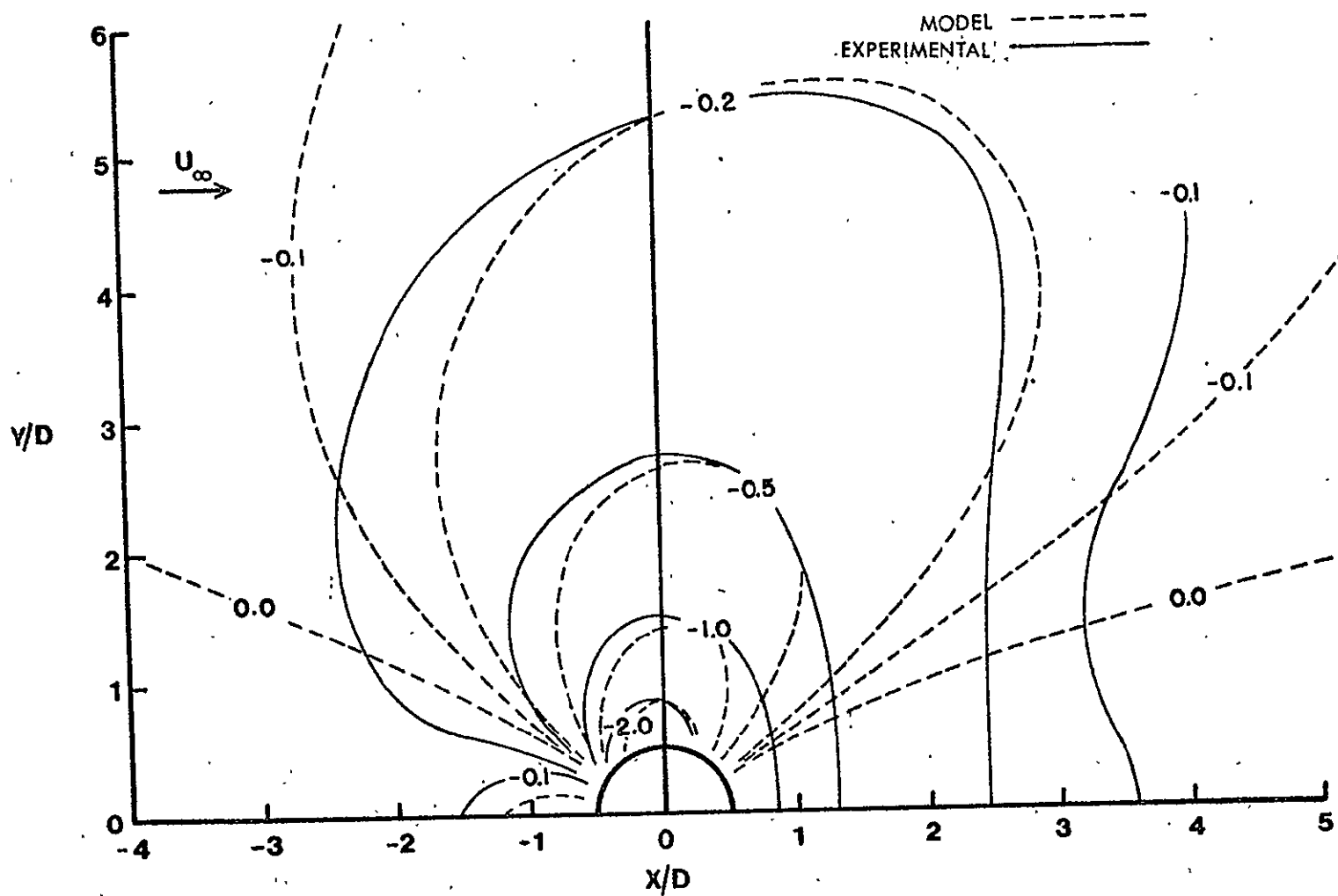


Figure 8. Comparison of Model Results with Experimental Pressure Contours for Zero Entrainment

○ RIGHT HALF-PLANE ( $\theta$ )  
 △ LEFT HALF-PLANE ( $-\theta$ )  
 MODEL ———

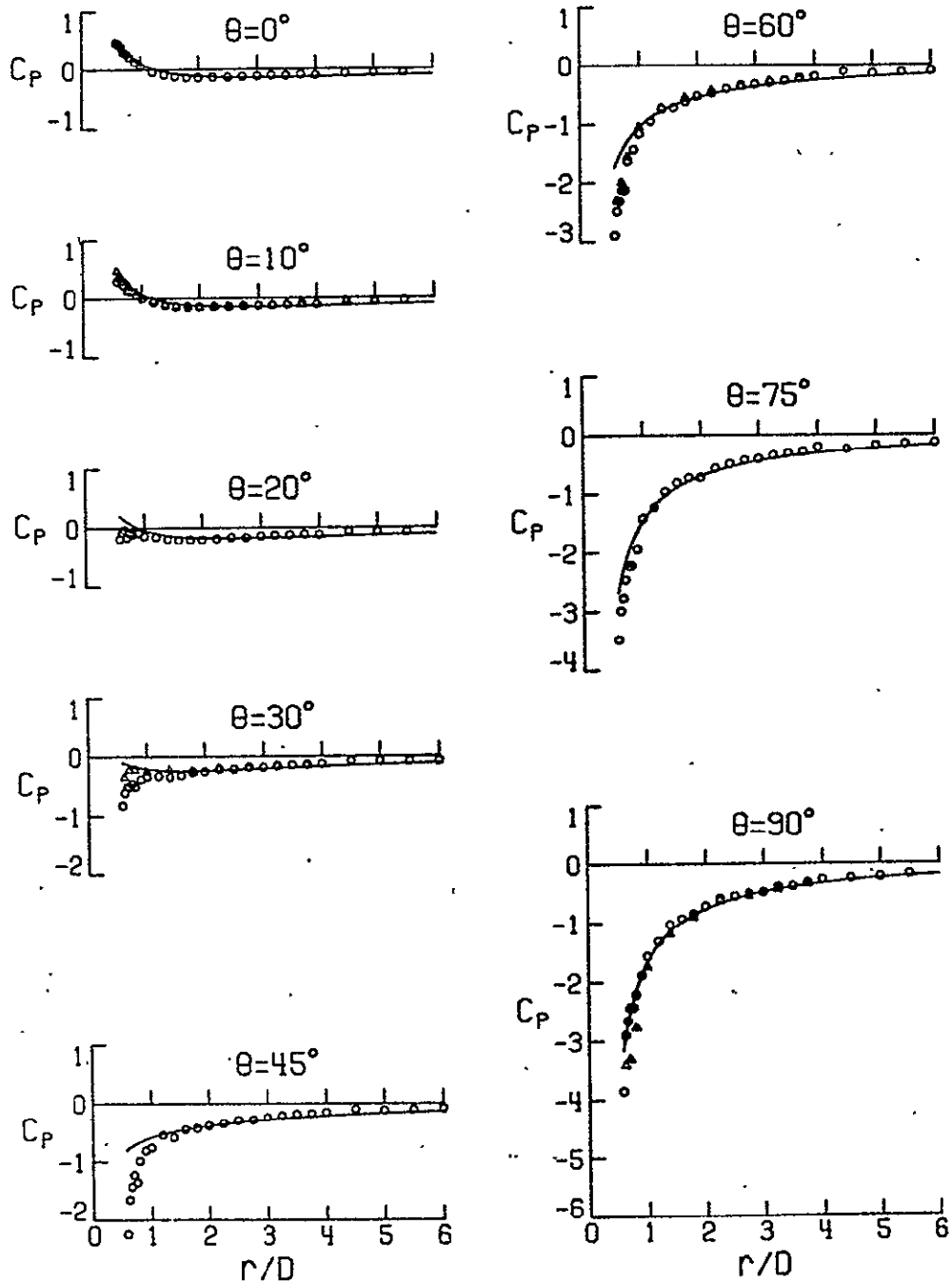


Figure 9. Comparison of Model Results with Experimental Pressure Coefficients for  $E=0.6$  ( $0^\circ < \theta < 90^\circ$ )



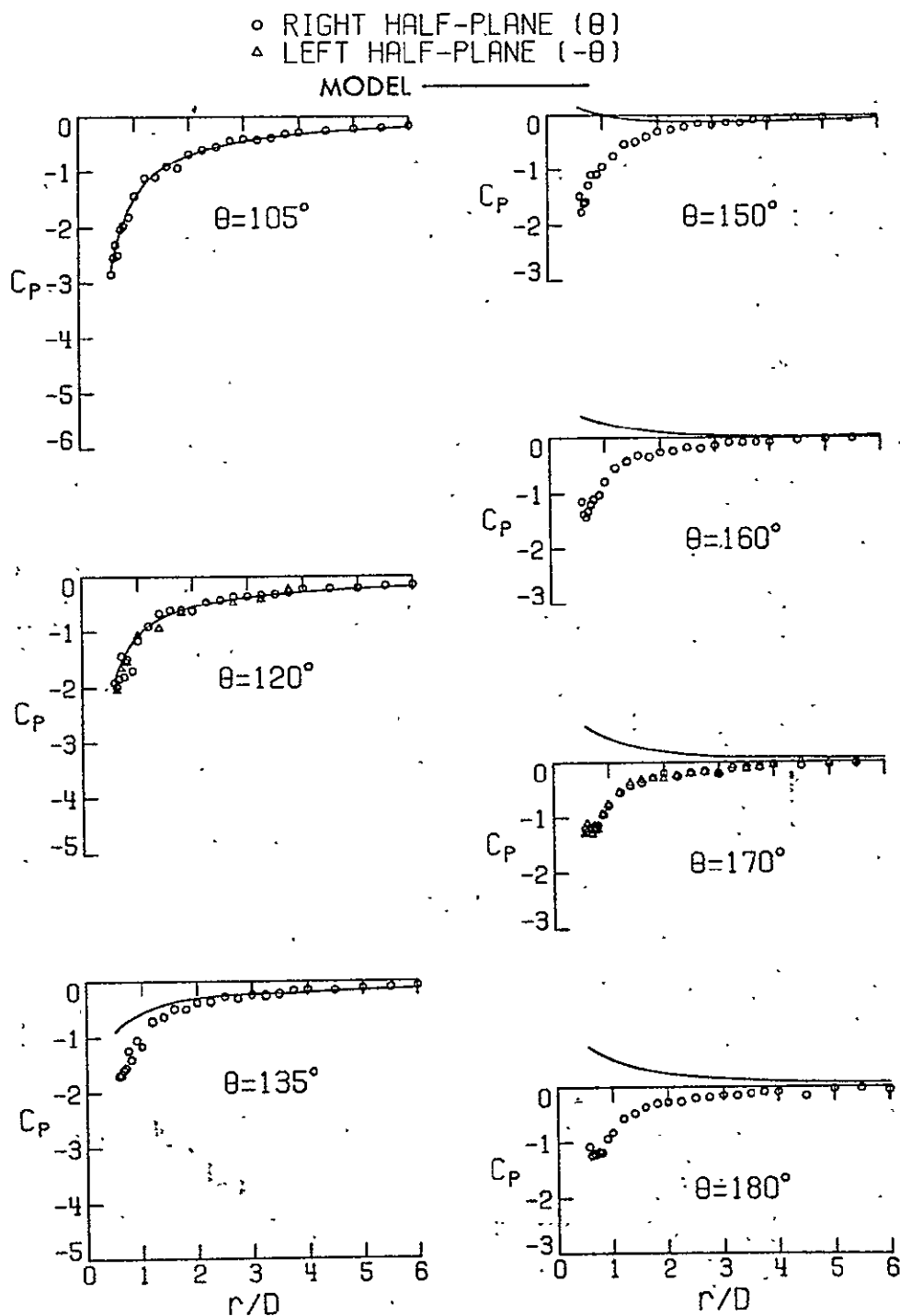


Figure 10. Comparison of Model Results with Experimental Pressure Coefficients for  $E=0.6$  ( $105^\circ < \theta < 180^\circ$ )

REPRODUCIBILITY OF THE  
ORIGINAL PAGE IS POOR

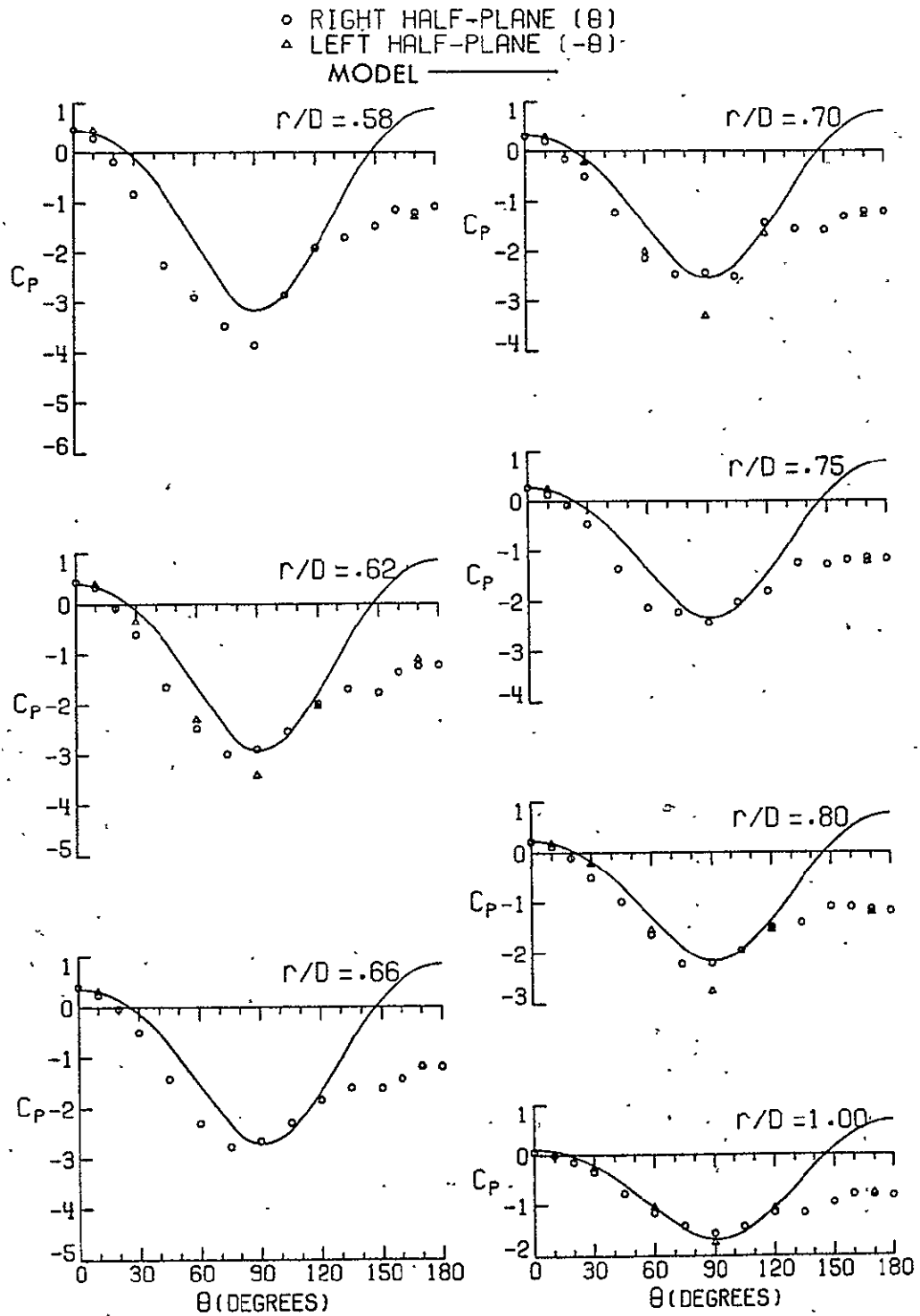


Figure 11. Comparison of Model Results with Experimental Pressure Coefficients for  $E=0.6$  ( $.58 < r/D < 1.00$ )

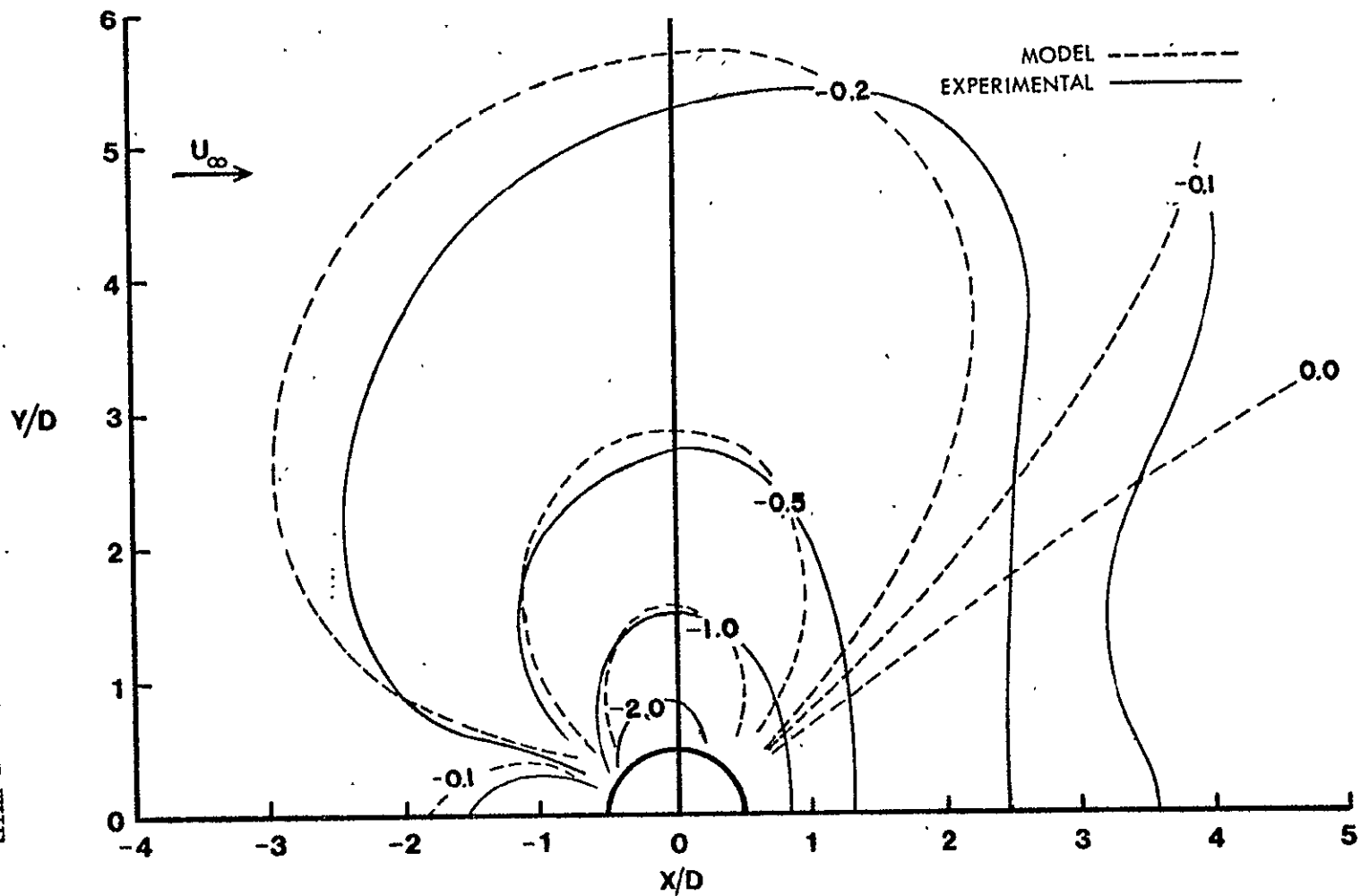


Figure 12. Comparison of Model Results with Experimental Pressure  
Contours for  $E=0.6$

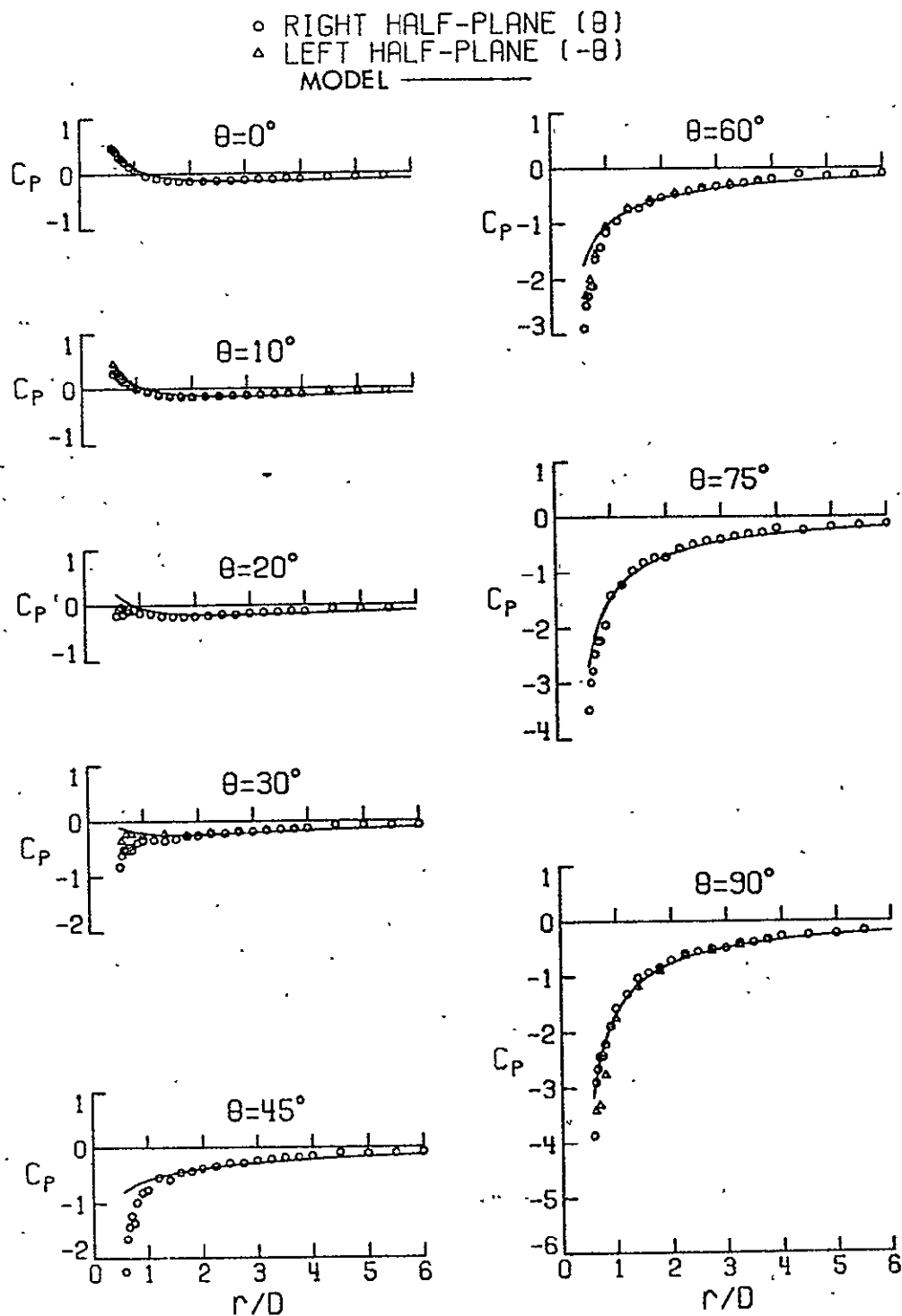


Figure 13. Comparison of Model Results with Experimental Pressure Coefficients with Application of Wake Region Considerations ( $E=0.6$ ,  $0^\circ < \theta < 90^\circ$ )

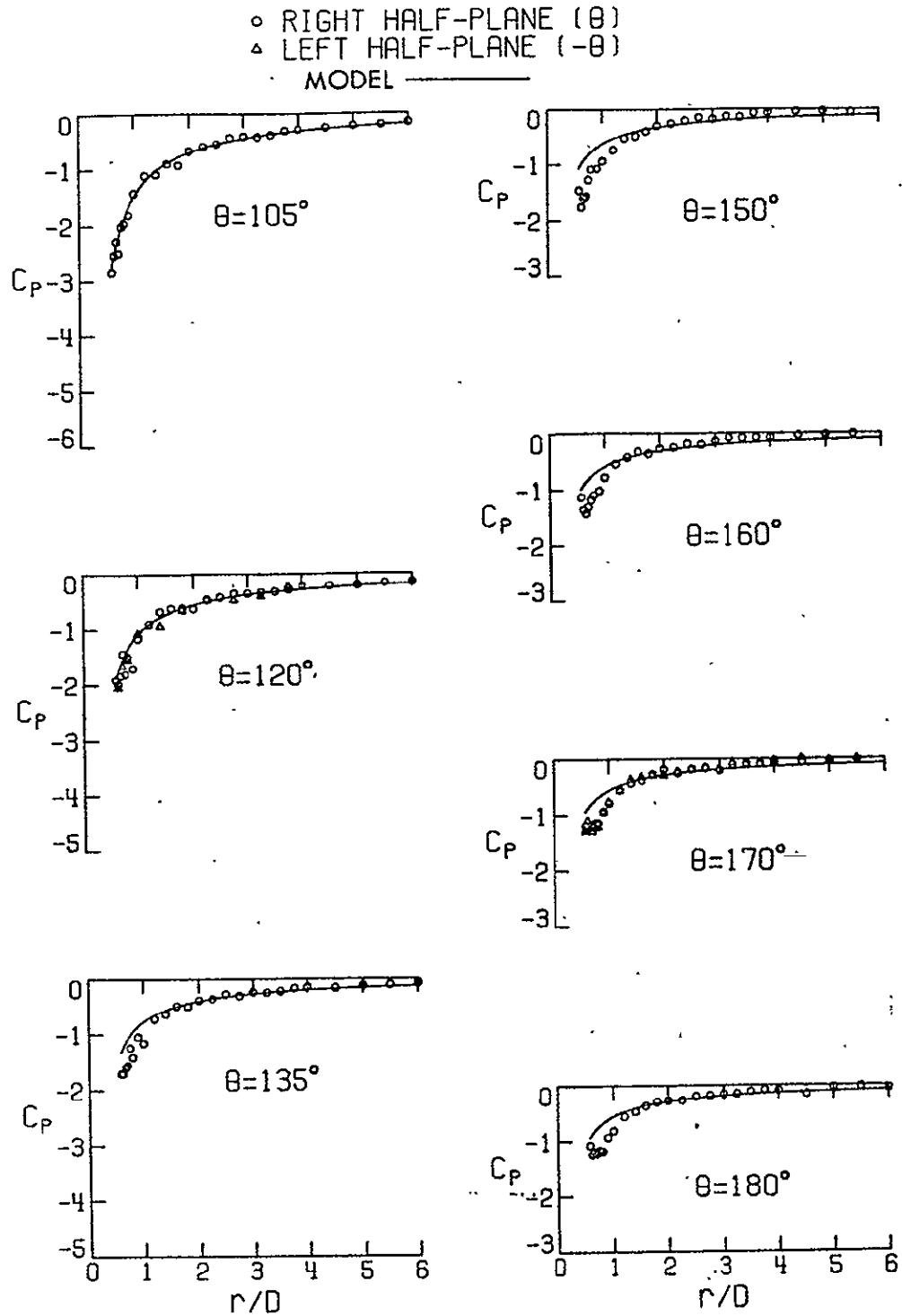


Figure 14. Comparison of Model Results with Experimental Pressure Coefficients with Application of Wake Region Considerations ( $E=0.6$ ,  $105^\circ < \theta < 180^\circ$ )

○ RIGHT HALF-PLANE ( $\theta$ )  
 △ LEFT HALF-PLANE ( $-\theta$ )  
 MODEL ———

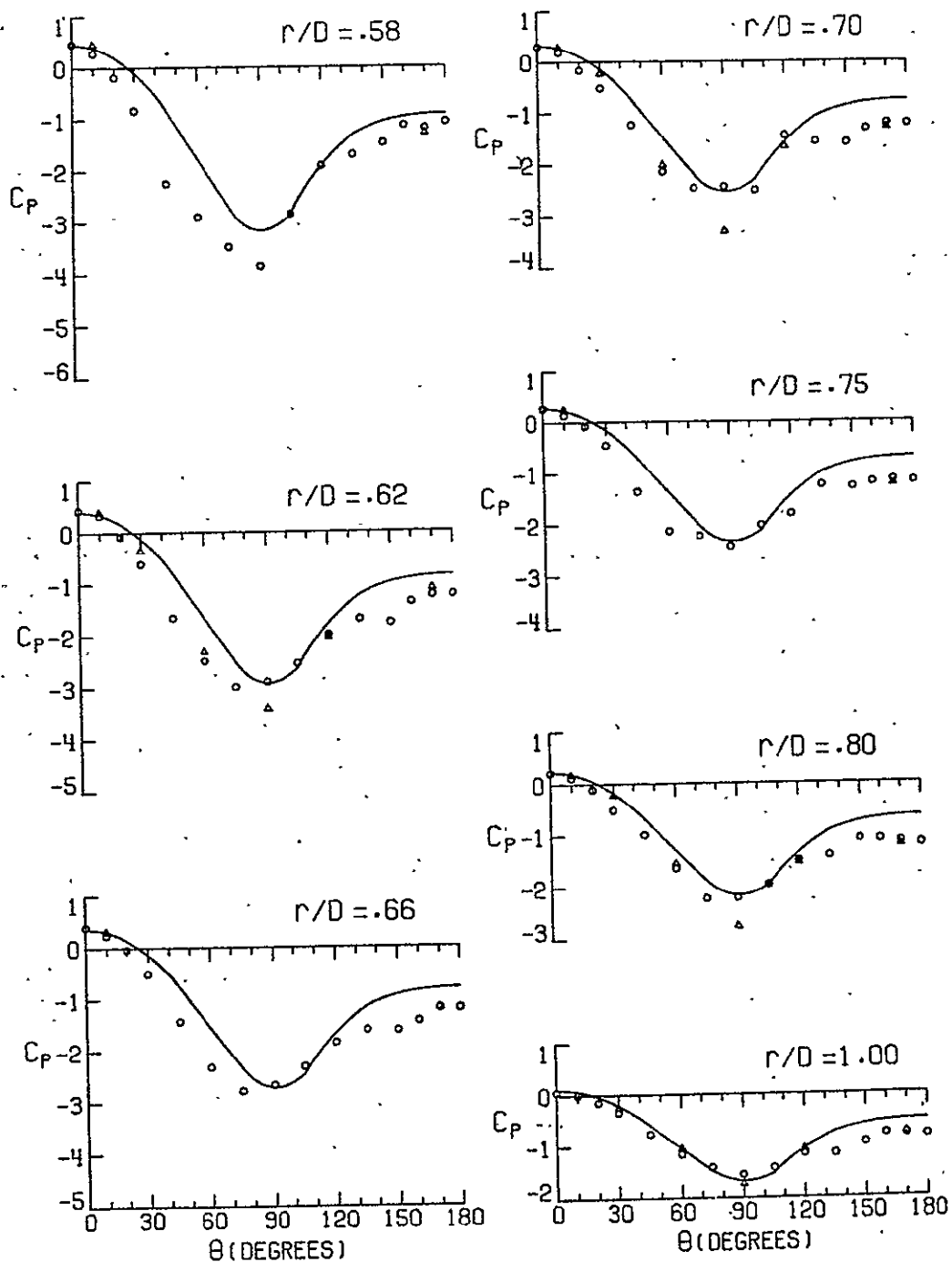


Figure 15. Comparison of Model Results with Experimental Pressure Coefficients with Application of Wake Region Considerations ( $E=0.6$ ,  $.58 < r/D < 1.00$ )

REPRODUCIBILITY OF THE  
 ORIGINAL PAGE IS POOR

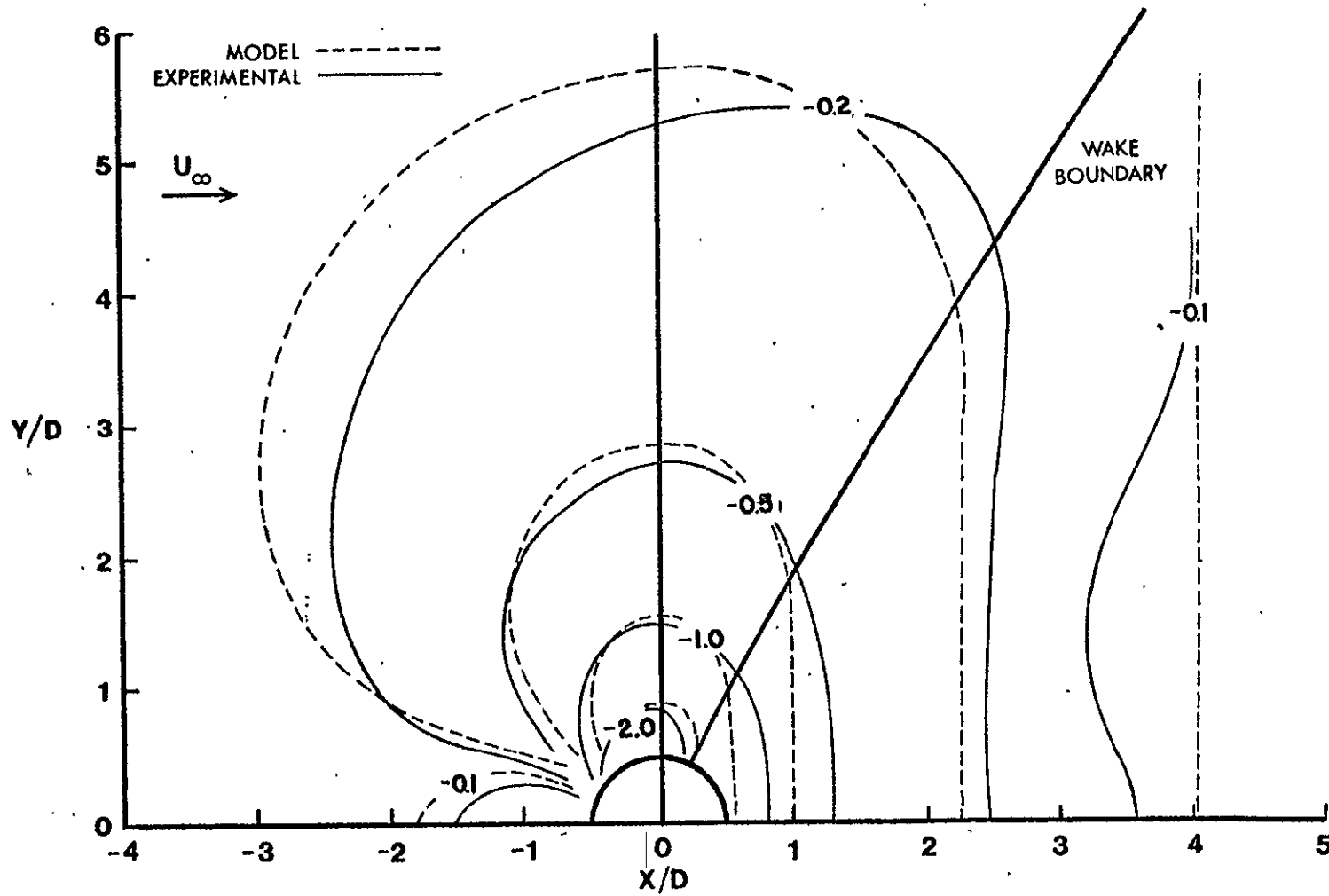


Figure 16. Comparison of Model Results with Experimental Pressure Contours with Application of Wake Region Considerations ( $E=0.6$ )

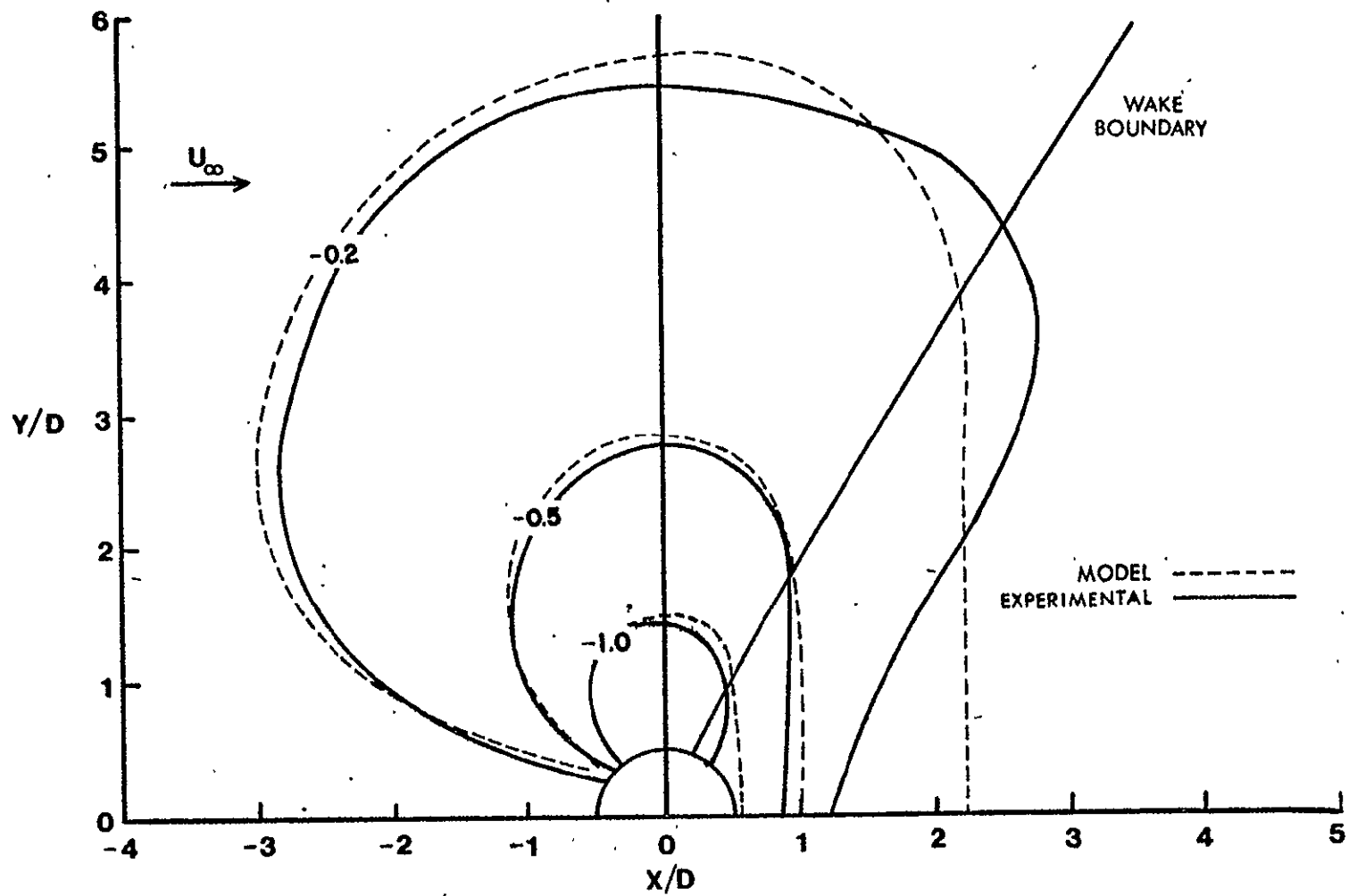


Figure 17. Comparison of Model Results with Results of Thompson (ref. 4)



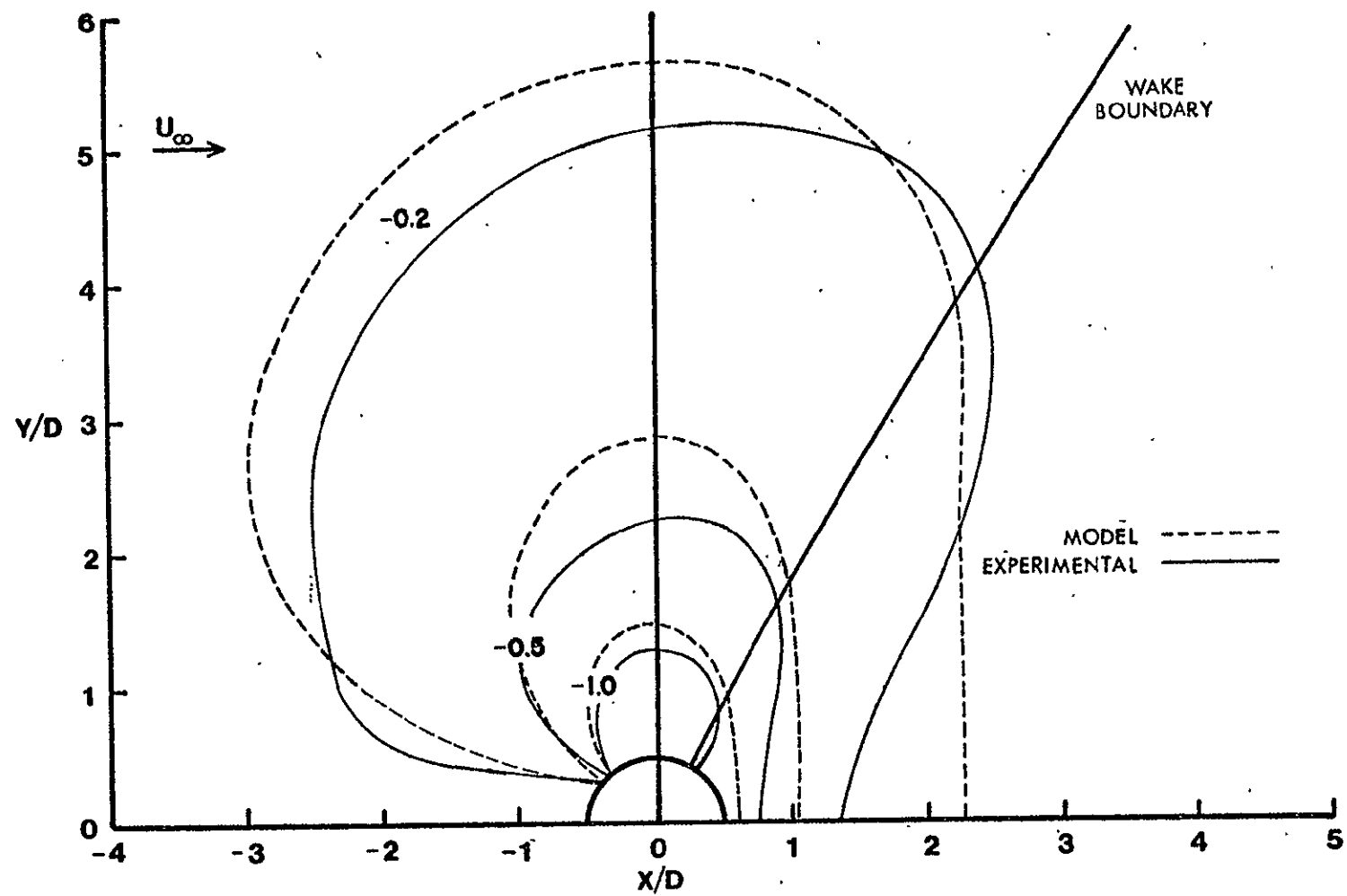


Figure 18. Comparison of Model Results with Results of Bradbury and Wood (ref. 5)

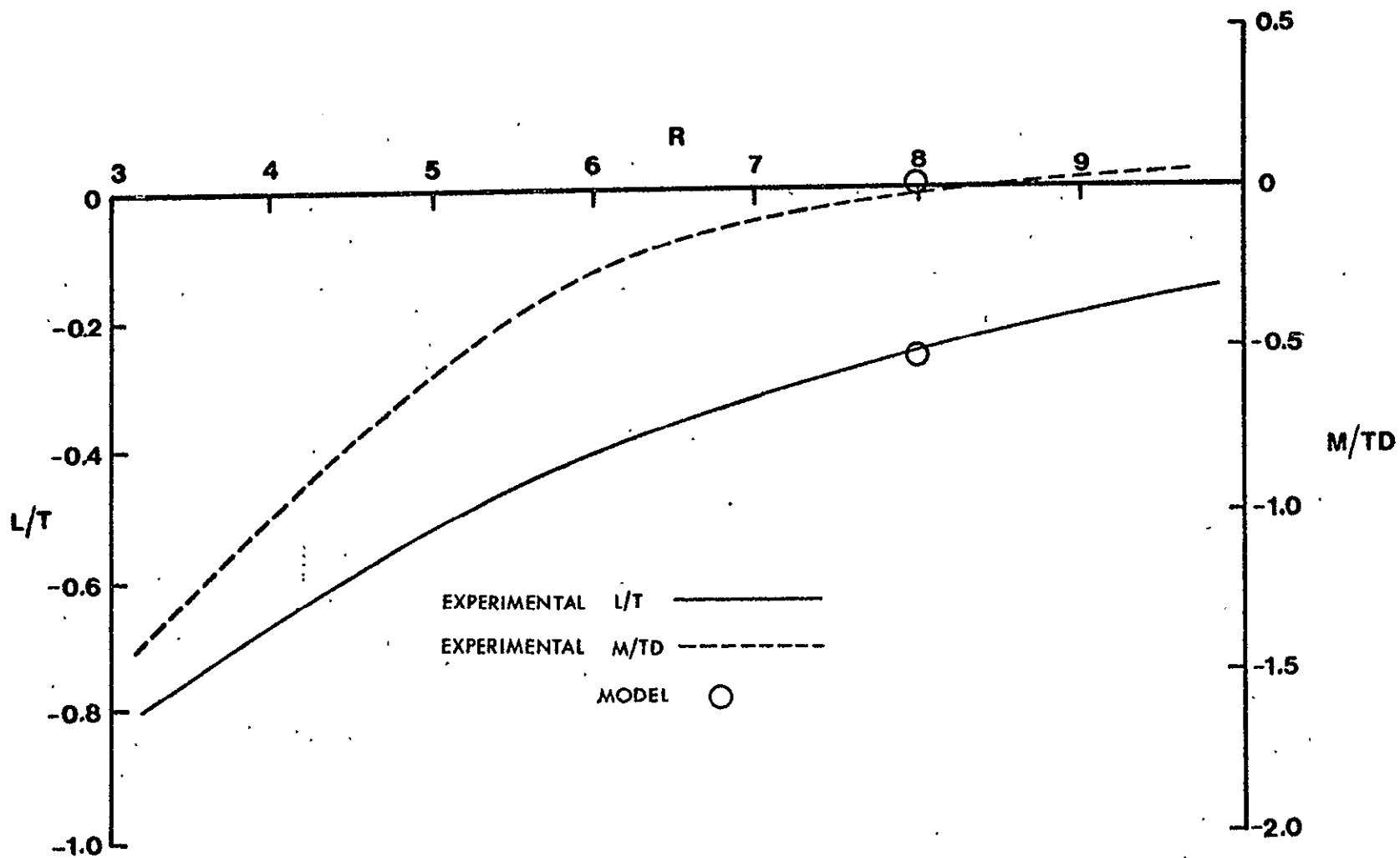


Figure 19. Comparison of Model Results and Experimental Lift and Moment on the Flat Plate

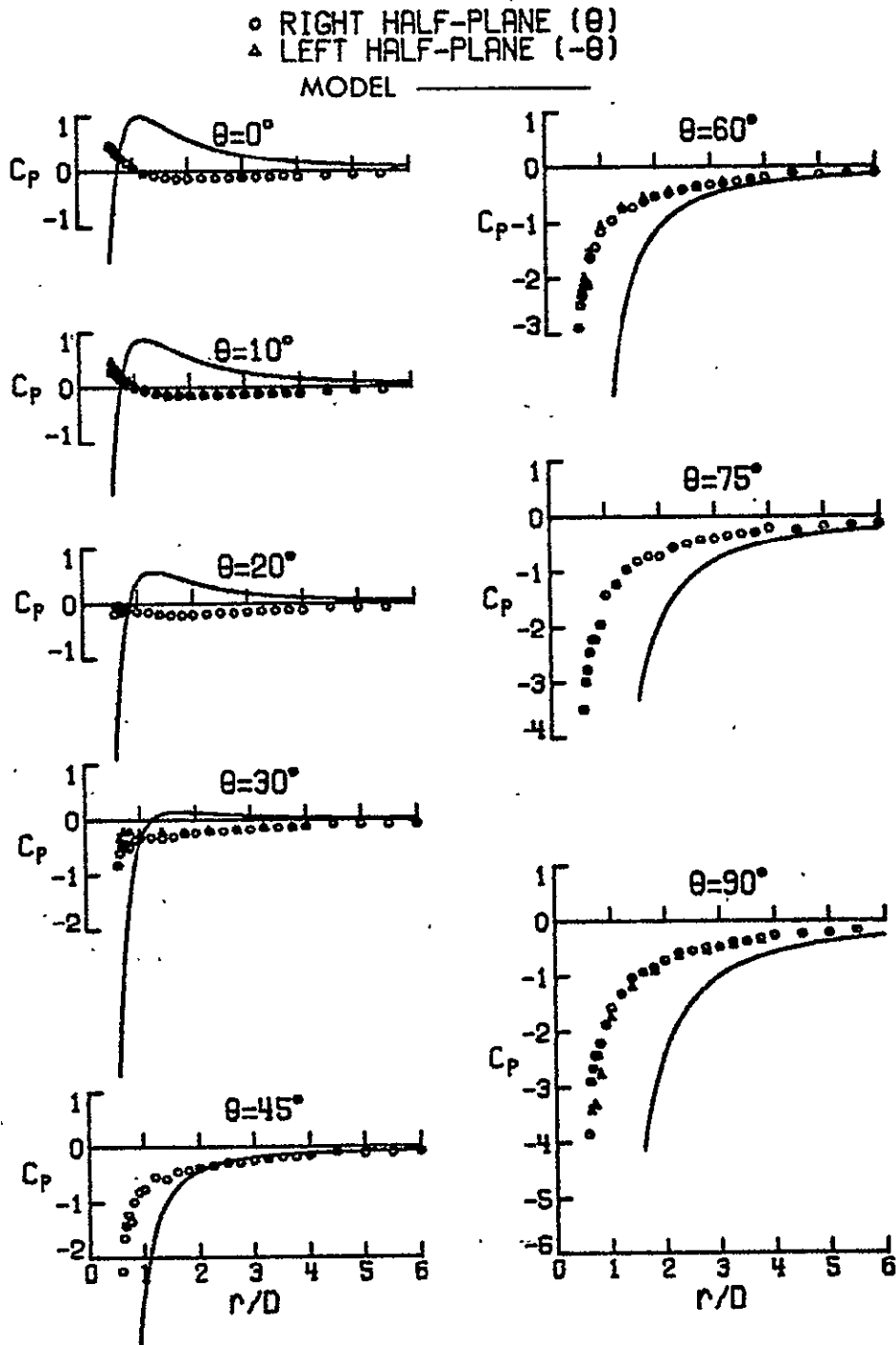


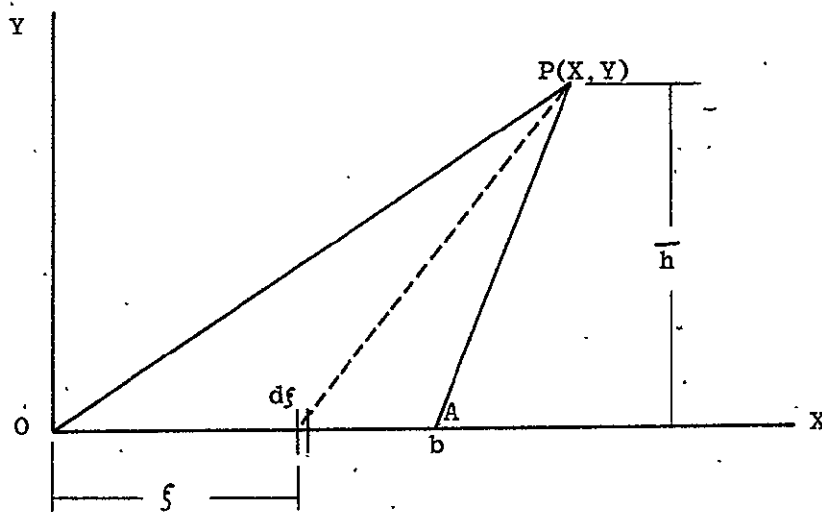
Figure 20. Comparison of Model Results and Experimental Pressure Coefficients (Vortices Begin at Edges of Jet Orifice)

## APPENDICES

# APPENDIX I

## Derivation of Finite Filament Sink (Source) Flow

The computer model institutes a distribution of finite filament sinks along the jet centerline. It is necessary to formulate an expression relating the sink filament strength and length to the induced velocity at a field point. Consider a distribution of equal strength sinks along the X-axis of a local coordinate system. (The axes used in this derivation should not be confused with the tunnel coordinate system described in the main text.)



The velocity potential induced by the infinitesimal element  $df$  is

$$d\phi = -\frac{g}{4\pi} \frac{df}{[(x-f)^2 + y^2]^{1/2}}$$

The total velocity potential induced by a line sink of length  $b$

may be written

$$\phi = -\frac{q}{4\pi} \int_0^b \frac{df}{[(x-f)^2 + y^2]^{1/2}}$$

The X-velocity induced may be found by the expression

$$\begin{aligned} U_x &= -\frac{\partial \phi}{\partial x} = \frac{\partial}{\partial x} \left[ \frac{q}{4\pi} \int_0^b \frac{df}{[(x-f)^2 + y^2]^{1/2}} \right] \\ &= \frac{q}{4\pi} \int_0^b \frac{\partial}{\partial x} \left[ \frac{df}{[(x-f)^2 + y^2]^{1/2}} \right] \end{aligned}$$

Therefore

$$U_x = -\frac{q}{4\pi} \int_0^b \frac{(x-f) df}{[(x-f)^2 + y^2]^{3/2}}$$

Let

$$x-f = \eta$$

$$df = -d\eta$$

$$U_x = \frac{q}{4\pi} \int_x^{x-b} \frac{\eta d\eta}{[\eta^2 + y^2]^{3/2}} = \frac{q}{4\pi} \left[ \frac{-1}{[(x-b)^2 + y^2]^{1/2}} - \frac{-1}{[x^2 + y^2]^{1/2}} \right]$$

$$= -\frac{q}{4\pi} \left[ \frac{1}{AP} - \frac{1}{OP} \right]$$

Similarly

$$U_y = -\frac{\partial \phi}{\partial y} = -\frac{\partial}{\partial y} \left[ -\frac{q}{4\pi} \int_0^b \frac{df}{[(x-f)^2 + y^2]^{1/2}} \right]$$

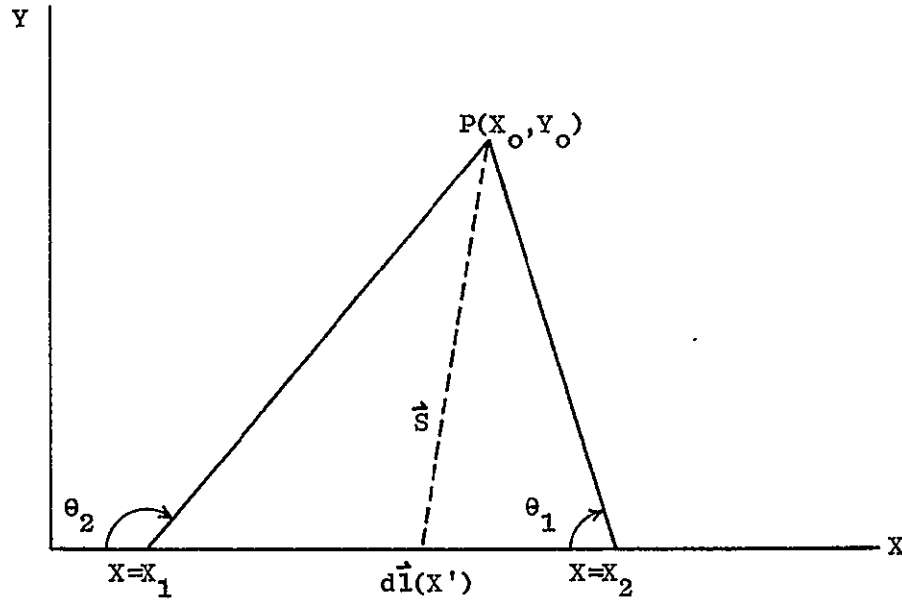
$$\begin{aligned}
&= -\frac{q}{4\pi} \int_0^b \frac{y \, d\xi}{[(x-\xi)^2 + y^2]^{3/2}} \\
&= \frac{q}{4\pi y} \left[ \frac{x-b}{[(x-b)^2 + y^2]^{1/2}} - \frac{x}{[x^2 + y^2]^{1/2}} \right] \\
&= \frac{q}{4\pi h} [\cos \alpha_2 - \cos \alpha_1]
\end{aligned}$$

The problem essentially reduces to a two dimensional geometrical analysis. When the endpoints of the filament and the field point are defined, the values of AP, OP, h,  $\alpha_1$ , and  $\alpha_2$  may be found through planar geometry. The projections of  $U_x$  and  $U_y$  onto the flat plate will yield the velocity on the flat plate which is induced by the finite filament.

## APPENDIX II

### Derivation of Finite Filament Vortex Flow

The computer model institutes a distribution of finite filament vortices along the vortex trajectories. Although the vortex endpoints and the field points are specified in three dimensions, the problem is two dimensional as far as calculating the induced velocities on the flat plate is concerned. Consider a filament vortex aligned along the X-axis of a local coordinate system (not to be confused with the tunnel oriented coordinate system). The X-Y plane contains the field point and the two vortex endpoints.



The general equation for the velocity induced by a filament vortex is

$$\vec{U} = -\frac{\Gamma}{4\pi} \oint \frac{\vec{S} \times d\vec{l}(x')}{S^3}$$

where  $\Gamma$  is the strength of the vortex. In vector form the terms



in the general equation become

$$\vec{S} = (x_0 - x') \vec{i} + y_0 \vec{j}$$

$$d\vec{\ell}(x') = dx' \vec{i}$$

$$\vec{S} \times d\vec{\ell}(x') = y_0 dx' \vec{k}$$

Let

$$\eta = x_0 - x'$$

$$y_0 = h$$

Therefore

$$\vec{U} = \frac{\Gamma}{4\pi} \int_{x_0 - x_2}^{x_0 - x_1} \frac{\eta d\eta}{[\eta^2 + h^2]^{3/2}} \vec{k}$$

$$= \frac{\Gamma}{4\pi h} \left[ \frac{x_0 - x_2}{[(x_0 - x_2)^2 + h^2]^{1/2}} - \frac{x_0 - x_1}{[(x_0 - x_1)^2 + h^2]^{1/2}} \right] \vec{k}$$

$$= \frac{\Gamma}{4\pi h} [\cos \theta_1 - \cos \theta_2] \vec{k}$$

If the field point and the endpoints of the vortex filament are defined, the parameters  $h$ ,  $\theta_1$ , and  $\theta_2$  may be found through the use of planar geometry. The projection of  $U$  onto the plane of the flat plate will equal the velocity induced on the flat plate by the filament vortex segment.

### APPENDIX III

#### COMPUTER PROGRAM FOR CALCULATING PRESSURE DISTRIBUTION ON FLAT PLATE

C  
C  
C  
C

THIS PROGRAM CALCULATES THE PRESSURE COEFFICIENTS ON THE FLAT  
PLATE INDUCED BY A JET ISSUING NORMALLY INTO A CROSSFLOW.

DIMENSION X(200),Y(200),Z(200),CP(200),S(200)

DIMENSION RAD(26),THETA(15)

DIMENSION P(26,15)

COMMON/ONE/GAM,CONPT,CONST

COMMON/TWO/RAD,THETA,P

COMMON/THREE/X,Z,S,N

COMMON/FOUR/X0,Y0,Z0,X1,Y1,Z1,X2,Y2,Z2,VXTOT,VYTOT,VZTOT

COMMON/FIVE/NOFIL,R,VJX,VJY,VJZ

INTEGER OPTION

COMMON/SIX/OPTION

DATA RAD/0.58,0.62,0.66,0.70,0.75,0.80,0.90,1.00,1.20,1.40,1.60,  
11.80,2.00,2.25,2.50,2.75,3.00,3.25,3.50,3.75,4.00,4.50,5.00,5.50,  
26.00,7.00/

DATA THETA/0.0,10.0,20.0,30.0,45.0,60.0,75.0,90.0,105.0,120.0,  
135.0,150.0,160.0,170.0,180.0/

AE=00.3473

BE=1.127

CE=0.4291

DIA=0.33333

U=127.0

READ (5,66) OPTION

C  
C  
C  
C

IF OPTION=1, THE VORTICES START FROM THE CENTER OF THE JET ORIFICE.

IF OPTION=2, THE VORTICES START FROM THE EDGES OF THE JET ORIFICE.

READ (5,65) NOFIL

READ(5,24) R

NOWAKE=1

C  
C

IF NCWAKE EQUALS 1, SUBROUTINE WAKE IS CALLED.

```

C      NOSINK=1
C
C      IF NOSINK EQUALS 1, A SYSTEM OF LINE SINKS IS GENERATED ALONG THE JET
C      CENTERLINE. OTHERWISE, NO JET ENTRAINMENT IS ACCOUNTED FOR.
C
      GAM=0.0
      DO 1100 M=1,15
      DO 1100 K=1,26
      P(K,M)=1E6
1100  CONTINUE
      N=NOFIL
      CALL ENDPT
      CP(1)=0.0
      IF (OPTION.EQ.1) CONST=2.04
      IF (OPTION.EQ.2) CONST=1.389
      DO 17 M=1,15
      DO 17 K=1,26
      ARC=0.0
      THET=THETA(M)*3.1416/180.0
C
C      DEFINE FIELD POINTS.
C
      XO=-RAD(K)*COS(THET)
      YO=RAD(K)*SIN(THET)
      ZO=0.0
      VXTO=0.0
      VYTO=0.0
      VZTO=0.0
      IF(OPTION.EQ.1) Y(1)=0.0
      IF(OPTION.EQ.2) Y(1)=0.5
      IF (NOWAKE.EQ.1.AND.THETA(M).GT.90) CALL WAKE(K,M)
C
C      DO LOOP 1 GENERATES A SERIES OF VORTEX FILAMENT SEGMENTS IN ORDER

```

C TO APPROXIMATE A CURVED VORTEX FILAMENT.

C

```

DO 1 I=1,N
X1=X(I)
X2=X(I+1)
SEG=S(I)
ARC=ARC+S(I)
CP(I+1)=ARC+S(I+1)/2.0
CONPT=CP(I)
HO=CONST*(1.-EXP(-ARC/8.0))
IF (OPTION.EQ.2) HO=HO+0.5
BD=2.11/SQRT(ARC)
ETA=BD*HO
Y(I+1)=HO/ERF(ETA)
Y1=Y(I)
Z1=Z(I)
Y2=Y(I+1)
Z2=Z(I+1)

```

C

C

C

DO LOOP 4 GENERATES TWO OBSERVED VORTICES AND TWO IMAGE VORTICES.

```

DO 4 J=1,4
IF(Z0.EQ.0.0.AND.J.GE.3) GO TO 4
GO TO (9,6,7,6),J
6 Y1=-Y1
Y2=-Y2
GO TO 9
7 Z1=-Z1
Z2=-Z2
9 CONTINUE

```

C

C

C

CALCULATE DISTANCES FROM VORTEX SEGMENT ENDPOINTS TO FIELD POINTS.

```

A=SQRT((X1-X0)**2+(Y1-Y0)**2+(Z1-Z0)**2)

```

```

      B=SQRT((X2-X0)**2+(Y2-Y0)**2+(Z2-Z0)**2)
      C=SQRT((X2-X1)**2+(Y2-Y1)**2+(Z2-Z1)**2)
      T=(A+B+C)/2.
      BMOUT=T*(T-A)*(T-B)*(T-C)
      IF (BMOUT.LT.0.0) GO TO 502
      E=SQRT(BMOUT)
      GO TO 503
502 E=0.01
503 CONTINUE

C
C      H= PERPENDICULAR DISTANCE FROM VORTEX FILAMENT TO FIELD POINT.
C
      H=2.*E/C
      H=H*DIA
      IF (H.LT..001) H=.001
      COS1=(A**2+C**2-B**2)/(2.0*A*C)
      COS2=(A**2-B**2-C**2)/(2.0*B*C)
      IF (R.EQ.8.0) CALL GAMMA8
      G1=2.0*GAM*U*DIA
      IF (I.EQ.N) COS2=-1

C
C      FIND MAGNITUDE OF VELOCITY INDUCED AT FIELD POINT BY VORTEX SEGMENT.
C
      V=G1*(COS1-COS2)/(4.0*3.1416*H)

C
C      CALCULATE VECTOR COMPONENTS FROM CROSS PRODUCT OF VECTOR A AND VECTOR B.
C
      AC=(Z1-Z0)*(Y2-Y0)-(Z2-Z0)*(Y1-Y0)
      BC=(X1-X0)*(Z2-Z0)-(X2-X0)*(Z1-Z0)
      CC=(Y1-Y0)*(X2-X0)-(X1-X0)*(Y2-Y0)
      GO TO (14,15,14,15),J
15 CONTINUE
      AC=-AC
      BC=-BC

```

CC=-CC  
14 CONTINUE

C  
C FIND DIRECTION COSINES OF INDUCED VELOCITY VECTOR.  
C

D=SQR(AC\*\*2+BC\*\*2+CC\*\*2)  
DCOSA=AC/D  
DCOSB=BC/D  
DCOSC=CC/D

C  
C SUM INDUCED VELOCITIES.  
C

VXTO=VXTO+DCOSA\*V  
VYTO=VYTO+DCOSB\*V  
VZTO=VZTO+DCOSC\*V

4 CONTINUE

1 CONTINUE

IF(ZO.EQ.0.0) VXTO=2.0\*VXTO  
IF(ZO.EQ.0.0) VYTO=2.0\*VYTO  
IF(ZO.EQ.0.0) VZTO=0.0  
VJX=0.0  
VJY=0.0  
VJZ=0.0  
IF (NOSINK.EQ.1) CALL JET

C  
C ADD VELOCITIES INDUCED BY SINK FILAMENT SEGMENTS.  
C

VXTO=VXTO+VJX  
VYTO=VYTO+VJY  
VZTO=VZTO+VJZ  
VXTO=VXTO+U

C  
C FIND TOTAL VELOCITY AND PRESSURE COEFFICIENT ON THE FLAT PLATE.  
C

```

      VTOT=SQRT(VXTO**2+VYTO**2+VZTO**2)
      P(K,M)=1.0-(VTOT**2.0)/(U**2.0)
17  CONTINUE
      CALL EXPCP
      CALL PRIMAT
      CALL LIFT
24  FORMAT(F5.2)
65  FORMAT (I3)
66  FORMAT (I1)
      STOP
      END
      SUBROUTINE ENDPT

```

C  
C  
C  
C

SUBROUTINE ENDPT GENERATES ENDPOINTS IN X AND Z FOR EACH VORTEX SEGMENT.

```

      COMMON/THREE/X(200),Z(200),S(200),N
      AE=0.3473
      BE=1.127
      CE=0.4291
      R=8.0
      A1=CE*AE*(R**BE)
      Z(1)=0.0
      Z(2)=.025
      X(1)=(Z(1)/(AE*(R**BE)))*(1.0/CE)
      X(2)=(Z(2)/(AE*(R**BE)))*(1.0/CE)
      S(1)=((X(2)-X(1))**2.0+(Z(2)-Z(1))**2.0)**0.5
      SCNE=2.0*S(1)
      NN=N+1
      TOTARC=0.0
      DO 100 I=2,NN
      DZ=A1*(X(I)**(CE-1.0))
      PHI=ATAN(DZ)
      X(I+1)=SCNE*COS(PHI)+X(I)

```



```

      Z(I+1)=AE*(R**BE)*(X(I+1))**CE
C
C      CALCULATE LOCAL RADIUS OF CURVATURE.
C
      RADCUR=(1.08375*(X(I)**1.047267)*(1.+2.41041*(X(I)**(-1.1418)))**
11.5
      S(I)=SQRT((X(I+1)-X(I))**2+(Z(I+1)-Z(I))**2)
      TOTARC=TOTARC+S(I)
C
C      CALCULATE LENGTH OF NEXT FILAMENT BASED ON RADIUS OF CURVATURE.
C
      IF(TOTARC.GT.1.00) SONE=RADCUR/50.
      WRITE(6,101) TOTARC,RADCUR,SONE
101  FORMAT(5X,'TOTARC,RADCUR,SONE =',3F10.4)
100  CONTINUE
      RETURN
      END
      SUBROUTINE JET
C
C      SUBROUTINE JET INSTITUTES A SERIES OF LINE SINKS ALONG THE JET
C      CENTERLINE IN ORDER TO ACCOUNT FOR MASS ENTRAINMENT BY THE JET.
C
      DIMENSION X(200),Z(200),CP(200),S(200)
      COMMON/FOUR/X0,Y0,Z0,AZ,BZ,CZ,ZZ,EZ,FZ,HARPO,ZEPPO,GROUCH
      COMMON/FIVE/NOFIL,R,VJX,VJY,VJZ
      COMMON/SEVEN/E,SCRIT
      CP(1)=0.0
      AE=0.9772
      BE=0.9113
      CE=0.3346
      U=127.0
      DIA=.3333
      PI=3.14159
C

```

C 'E' IS THE ENTRAINMENT COEFFICIENT. 'SCRIT' IS THE CRITICAL LENGTH FOR  
C ESTABLISHMENT OF THE JET FLOW.  
C

E=0.6  
SCRIT=3.0

C  
C GENERATE THE ENDPOINTS OF THE SINK FILAMENT SEGMENTS.  
C

XTOT=0.0  
ZTOT=0.0  
TOTARC=0.0  
Z(1)=0.0  
Z(2)=.025  
X(1)=(Z(1)/(AE\*(R\*\*BE)))\*\*(1.0/CE)  
X(2)=(Z(2)/(AE\*(R\*\*BE)))\*\*(1.0/CE)  
S(1)=((X(2)-X(1))\*\*2.0+(Z(2)-Z(1))\*\*2.0)\*\*0.5  
XTOT=X(2)-X(1)  
SONE=2.0\*S(1)  
NN=NOFIL+1  
ARCLTH=0.0  
DO 100 I=2,NN  
DZ=CE\*AE\*(R\*\*BE)\*(XTOT\*\*(CE-1.0))  
PHI=ATAN(DZ)  
X(I+1)=SONE\*COS(PHI)+XTOT  
Z(I+1)=AE\*(R\*\*BE)\*(X(I+1))\*\*CE  
S(I)=SQRT((X(I+1)-X(I))\*\*2+(Z(I+1)-Z(I))\*\*2)  
XTOT=X(I+1)  
ARCLTH=S(I)+ARCLTH

C  
C CALCULATE LOCAL RADIUS OF CURVATURE OF JET TRAJECTORY AND ADJUST LENGTH  
C OF NEXT SEGMENT ACCORDINGLY.  
C

IF(X(I).LT.0.001) GO TO 100  
RADCUR=1.4475\*(X(I)\*\*(-1.6654))/(1.+4.7315\*(X(I)\*\*(-1.3308)))\*\*1.5

```

RADCUR=1./RADCUR
IF (ARCLTH.GT.3.00) SONE=RADCUR/50.
100 CONTINUE
VJX=0.0
VJY=0.0
VJZ=0.0
DO 13 I=1,NOFIL
TOTARC=TOTARC+S(I)
CP(I+1)=TOTARC+S(I+1)/2.0
CONPT=CP(I)
X1=X(I)
X2=X(I+1)
Y1=0.0
Y2=0.0
Z1=Z(I)
Z2=Z(I+1)
DO 19 J=1,2
IF (Z0.EQ.0.0.AND.J.EQ.2) GO TO 19
IF (J.EQ.1) GO TO 21
Z1=-Z1
Z2=-Z2
21 CONTINUE

```

C  
C  
C

CALCULATE STRENGTH OF SINK FILAMENT SEGMENT.

```

UJET=R*U
Q0=UJET*(PI*(DIA**2)/4.0)
IF (CONPT.LE.SCRIT) Q=E*CONPT*Q0/(SCRIT*DIA)
IF (CONPT.GT.SCRIT) Q=E*Q0/DIA

```

C  
C  
C  
C

CALCULATE THE DISTANCES FROM THE ENDPOINTS TO THE FIELD POINT AND THE HEIGHT OF THE RESULTING TRIANGLE.

```

PA=SQRT((X0-X1)**2+(Y0-Y1)**2+(Z0-Z1)**2)

```

```

PB=SQRT((X0-X2)**2+(Y0-Y2)**2+(Z0-Z2)**2)
AB=SQRT((X1-X2)**2+(Y1-Y2)**2+(Z1-Z2)**2)
SL=(PA+PB+AB)/2.0
ARZ=SL*(SL-PA)*(SL-PB)*(SL-AB)
IF (ARZ.LE.0.0) GO TO 301
AK=SQRT(ARZ)
QP=2.0*AK/AB
GO TO 302
301 QP=.01
302 CONTINUE
AQ=SQRT((PA**2.0)-(QP**2.0))
COS1=(PA**2+AB**2-PB**2)/(2.0*AB*PA)
COS2=(AB**2+PB**2+PA**2)/(2.0*AB*PB)
IF(COS1.GT.1.0) COS1=1.0
IF(COS1.LT.-1.0) COS1=-1.0
IF(COS2.GT.1.0) COS2=1.0
IF(COS2.LT.-1.0) COS2=-1.0
COS2=-COS2
ANG1=ARCOS(COS1)
ANG2=ARCOS(COS2)

C
C
C   CALCULATE THE DIRECTION COSINES OF THE FILAMENT SEGMENT.

COSALF=(X2-X1)/AB
COSBET=(Y2-Y1)/AB
COSGAM=(Z2-Z1)/AB

C
C
C   CALCULATE THE X, Y, AND Z CO-ORDINATES OF THE POINT OF INTERSECTION
C   OF THE PERPENDICULAR LINE FROM THE FIELD POINT TO THE FILAMENT.

IF (ANG1.LT.PI/2.) GO TO 11
IF (ANG1.GT.PI/2.) GO TO 10
11 XQ=X1+AQ*COSALF
   YQ=Y1+AQ*COSBET

```

```

      ZQ=Z1-AQ*COSEGAM
      GO TO 12
10  XQ=X1-AQ*COSEALF
      YQ=Y1-AQ*COSEBET
      ZQ=Z1-AQ*COSEGAM
12  CONTINUE

C
C      CALCULATE THE DIRECTION COSINES OF THE PERPENDICULAR LINE FROM
C      THE FILAMENT TO THE FIELD POINT.
C
      COSPHI=(X0-XQ)/QP
      COSOMG=(Y0-YQ)/QP
      COSZET=(Z0-ZQ)/QP
      QP=QP#DIA

C
C      CALCULATE THE VELOCITIES INDUCED BY THE FILAMENT SEGMENT AT THE
C      FIELD POINT.
C
      UY=Q*(COSZ-COS1)/(4.0*PI*QP)
      UX=Q*((1.0/PA)-(1.0/PB))/(4.0*PI)
      UX=UX/DIA
      VXSINK=UY*COSPHI
      VYSINK=UY*COSOMG
      VZSINK=UY*COSZET
      UXSINK=UX*COSEALF
      UYSINK=UX*COSEBET
      UZSINK=UX*COSEGAM

C
C      ADD THE RESULTING VELOCITY COMPONENTS.
C
      VJX=VXSINK+UXSINK+VJX
      VJY=VYSINK+UYSINK+VJY
      VJZ=VZSINK+UZSINK+VJZ
19  CONTINUE

```

```

13 CONTINUE
  IF(Z0.EQ.0.0) VJX=2.0*VJX
  IF(Z0.EQ.0.0) VJY=2.0*VJY
  IF(Z0.EQ.0.0) VJZ=0.0
  RETURN
  END
  SUBROUTINE GAMMA8

```

```

C
C  SUBROUTINE GAMMA8 SELECTS AN APPROPRIATE VORTEX STRENGTH
C  FOR EACH VORTEX FILAMENT FOR A VELOCITY RATIO OF 8.0 .
C

```

```

  COMMON/ONE/GAM,CONPT,CONST
  INTEGER OPTION
  COMMON/SIX/OPTION

```

```

C
C  *CONPT* IS THE DISTANCE ALONG THE VORTEX TRAJECTORY TO THE CONTROL POINT
C  OF THE VORTEX SEGMENT BEING ANALYZED.
C

```

```

  IF (CONPT.EQ.0.0) GO TO 103
  BD=2.110268/SQRT(CONPT)
  HO=CONST*(1.-EXP(-CONPT/8.0))
  IF(OPTION.EQ.2) HO=HO*0.5
  ETA=BD*HO
  GAM=0.72*8.0*ERF(ETA)
  GO TO 104
103 IF (OPTION.EQ.1) GAM=0.0
  IF(OPTION.EQ.2) GAM=5.76
104 CONTINUE
  RETURN
  END
  SUBROUTINE PRTMAT

```

```

C
C  SUBROUTINE PRTMAT PRINTS CALCULATED PRESSURE COEFFICIENTS,
C  EXPERIMENTAL PRESSURE COEFFICIENTS, THE DIFFERENCE BETWEEN

```

```

C      CALCULATED AND EXPERIMENTAL PRESSURE COEFFICIENTS, AND UNWEIGHTED
C      STANDARD DEVIATION.
C
C      DIMENSION DIFF(26,15)
C      COMMON/TWO/RAD(26),THETA(15),P(26,15)
C      COMMON/FIVE/NOFIL,R,HUP,TUP,THREEP
C      INTEGER OPTION
C      COMMON/SIX/OPTION
C      COMMON/SEVEN/E,SCRIT
C      COMMON/TEN/D(21,26)
C      DELPT=0.0
C      SUMDIF=0.0
C      DO 999 M=1,15
C      DO 999 K=1,26
C
C      CALCULATE DIFFERENCES IN EXPERIMENTAL AND THEORETICAL VALUES.
C
C      DIFF(K,M)=P(K,M)-D(M,K)
C      IF (ABS(DIFF(K,M)).GT.10) DIFF(K,M)=1E6
C      IF(DIFF(K,M).EQ.1E6) DELPT=DELPT+1.
C      IF(DIFF(K,M).EQ.1E6) GO TO 999
C      DIFF(K,M)=DIFF(K,M)**2
C      SUMDIF=SUMDIF+DIFF(K,M)
C
C      CALCULATE PERCENT DIFFERENCE FOR EACH POINT.
C
C      DIFF(K,M)=SQRT(DIFF(K,M))*100.
C      999 CONTINUE
C
C      CALCULATE UNWEIGHTED STANDARD DEVIATION.
C
C      STDEV=SQRT((SUMDIF/(390.-DELPT)))
C      WRITE(6,1011) NOFIL,R
C      WRITE(6,1013) E,SCRIT

```

```

      IF (CPTION.EQ.1) WRITE(6,1009)
      IF (OPTION.EQ.2) WRITE(6,1010)
      WRITE (6,1012)
      WRITE(6,1007)
      WRITE(6,1001)
      WRITE(6,1002) (RAD(K),K=1,13)
      WRITE(6,1001)
      WRITE(6,1006)
      DO 1004 M=1,15
      WRITE(6,1003) THETA(M),(P(K,M),K=1,13)
      WRITE(6,1014) (D(M,L),L=1,13)
      WRITE(6,1015) (DIFF(K,M),K=1,13)
1004 CONTINUE
      WRITE(6,1000)
      WRITE(6,1007)
      WRITE(6,1001)
      WRITE(6,1002) (RAD(K),K=14,26)
      WRITE(6,1001)
      WRITE(6,1006)
      DO 1005 M=1,15
      WRITE(6,1003) THETA(M),(P(K,M),K=14,26)
      WRITE(6,1014) (D(M,L),L=14,26)
      WRITE(6,1015) (DIFF(K,M),K=14,26)
1005 CONTINUE
      WRITE(6,1016) STDEV
1000 FORMAT(1H1,///,55X,21HPRESSURE COEFFICIENTS,///)
1001 FORMAT(1X,127(1H'))
1002 FORMAT(15X,13(F5.2,4X))
1003 FORMAT(3X,F4.0,2X,1H',5X,13(F7.3,2X))
1006 FORMAT(4X,'ANGLE',/)
1007 FORMAT(64X,'R/D')
1009 FORMAT(5X,'OPTION=1A, VORTICES START FROM CENTER OF JET ORIFICE.')
1010 FORMAT(5X,'OPTION=2A, VORTICES START FROM EDGE OF JET ORIFICE.')
1014 FORMAT(1X,'EXP. VALUES',3X,13(F7.3,2X))

```



```

1015 FORMAT(1X,'PCT. ERROR',4X,13(F7.3,2X),/)
1016 FORMAT(1H1,5X,'STANDARD DEVIATION =',F10.4,/)
1011 FORMAT (1H1,5X,I3,1X,'VORTEX AND SINK FILAMENT SEGMENTS ARE USED',
1/,5X,'VELOCITY RATIO =',F5.2,/)
1012 FORMAT (///,55X,'PRESSURE COEFFICIENTS',///)
1013 FORMAT(5X,'ENTRAINMENT COEFFICIENT =',F6.4,/,5X,'CRITICAL LENGTH
1 FOR JET FLOW ESTABLISHMENT =',F6.4,1X,'S/D')
RETURN
END
SUBROUTINE LIFT

```

```

C
C SUBROUTINE LIFT CALCULATES LIFT AND PITCHING MOMENTS ON THE FLAT
C PLATE FROM BOTH EXPERIMENTAL AND CALCULATED PRESSURE COEFFICIENTS.
C

```

```

DIMENSION AZIMTH(30)
COMMON/TWO/RAD(26),THETA(15),P(26,15)
COMMON/TEN/D(21,26)
RADIAN=3.14159265/180.0
GINF=19.935
VJ=0.1247
WP=6.66
WMACH=0.93
T=148.10
TE=(T+459.7)/(1.0+0.2*WMACH**2)

```

```

C
C CALCULATE THRUST OF JET.
C
THRUST=WP/32.17*WMACH*49.02*SQRT(TE)
EXLIFT=0.0
EXPPCH=0.0
DLIFT=0.0
PMOM=0.0
R=4.0
TAREA=0.0

```

```

DO 209 M=1,15
209  AZIMTH(M)=THETA(M)*RADIAN
    DO 210 K=1,23
    DO 210 M=1,14
    DTHETA=AZIMTH(M+1)-AZIMTH(M)

C
C  CALCULATE INCREMENTAL AREA.
C
C  AREA=R*R*(RAD(K+1)**2-RAD(K)**2)*DTHETA/2.

C
C  CALCULATE AVERAGE PRESSURE COEFFICIENTS OVER AREA.
C
C  CPAVG=(P(K,M)+P(K+1,M)+P(K,M+1)+P(K+1,M+1))/4.0
    DELFOR=CPAVG*QINF*AREA/144.0

C
C  CALCULATE MOMENT ARM.
C
C  PMARM=R*(RAD(K+1)+RAD(K))*COS(AZIMTH(M+1)-DTHETA/2.)/2.
    PMOM1=PMARM*DELFOR/12.

C
C  SUM LIFT OVER AREA.
C
C  DLIFT=DLIFT+DELFOR

C
C  SUM MOMENTS.
C
C  PMOM=PMOM+PMOM1

C
C  SUM AREA. NOTE TOTAL AREA INCLUDES ONE-HALF OF FLAT PLATE.
C
C  TAREA=TAREA+AREA

C
C  CALCULATE AVERAGE EXPERIMENTAL PRESSURE COEFFICIENTS AND SUM LIFT AND
C  MOMENTS.

```

```

C      EXPAVG=(D(M,K)+D(M+1,K)+D(M,K+1)+D(M+1,K+1))/4.0
      EXPFOR=EXPAVG*QINF*AREA/144.0
      EXPMOM=PMARM*EXPFOR/12.
      EXLIFT=EXLIFT+EXPFOR
      EXPPCH=EXPPCH+EXPMOM
210  CONTINUE

C      BY SYMMETRY, CALCULATE TOTAL LIFT, MOMENT, AND AREA BY MULTIPLYING ABOVE
C      RESULTS BY TWO.
C
C      DLIFT=2.0*DLIFT
      PMOM=2.0*PMOM
      TAREA=TAREA*2.0
      EXLIFT=2.0*EXLIFT
      EXPPCH=2.0*EXPPCH

C      NON-DIMENSIONALIZE LIFT AND MOMENTS.
C
C      EXLIFT=EXLIFT/THRUST
      EXPPCH=EXPPCH/(THRUST*0.3333)
      POVERT=DLIFT/THRUST
      TM=PMOM/(THRUST*0.3333)

C      CALCULATE WEIGHTED STANDARD DEVIATION.
C
C      TOTFOR=0.0
      TOTAR=0.0
      DO 211 M=1,15
      DO 211 K=1,25
      IF (M.EQ.15) THET2=180.0
      IF (M.NE.15) THET2=(THETA(M+1)+THETA(M))/2.
      RA2=(RAD(K+1)+RAD(K))/2.
      IF (K.EQ.1) RA1=0.50

```

```

      IF(M.EQ.1) THET1=0.0
      IF(K.NE.1) RAI=(RAD(K-1)+RAD(K))/2.
      IF(M.NE.1) THET1=(THETA(M-1)+THETA(M))/2.
      AREA1=R*R*(RA2**2-RA1**2)*(THET2-THET1)*RADIAN/2.
      CPDIFF=P(K,M)-D(M,K)
      IF(ABS(CPDIFF).GT.50.) GO TO 211
      FORDIF=(CPDIFF*AREA1)**2
      TOTFOR=TOTFOR+FORDIF
      TOTAR=AREA1**2+TOTAR
211  CONTINUE
      STDEV=SQRT(TOTFOR/TOTAR)
      WRITE(6,212) STDEV
      WRITE(6,3) THRUST
      WRITE(6,2) TAREA
      WRITE(6,1) POVERT,TM
      WRITE(6,4) EXLIFT,EXPPCH
212  FORMAT(5X,'WEIGHTED STANDARD DEVIATION =',F10.4,/)
      4  FORMAT(///,5X,'EXPERIMENTAL VALUES',/5X,'*****',
      1/,5X,'LIFT =',F10.4,/5X,'PITCHING MOMENT =',F10.4)
      1  FORMAT(5X,'TOTAL NON-DIMENSIONALIZED LIFT =',F10.4,/,5X,'TOTAL
      1 NON-DIMENSIONALIZED PITCHING MOMENT =',F10.4)
      2  FORMAT(5X,'TOTAL AREA =',F10.4,'SQUARE INCHES',/)
      3  FORMAT(5X,'THRUST =',F10.4)
      RETURN
      END
      SUBROUTINE EXPCP
C
C  SUBROUTINE EXPCP CONVERTS RAW DATA FROM SCANIVALVE PORTS TO VALUES
C  CORRESPONDING TO SPECIFIC FIELD POINTS SPECIFIED BY RADIUS AND ANGLE.
C
      COMMON/TEN/D(21,26)
      DIMENSION CP(10,46)
      DO 3 J=1,21
      DO 3 K=1,26

```

```

      3 D(J,K)=100.
C
C      READ EXPERIMENTAL DATA.
C
      READ(5,6) ((CP(I,J),I=1,10),J=1,45),(CP(I,46),I=1,9)
6  FORMAT(10F8.4)
      DO 50 J=1,20
      IF(J.GT.16) GO TO 50
      D(J,1)=CP(1,J)
      D(J,2)=CP(1,J+17)
      D(J,4)=CP(2,J+9)
      D(J,5)=CP(2,J+30)
      D(J,6)=CP(3,J+1)
      D(J,7)=CP(3,J+22)
      D(J,9)=CP(4,J+14)
      D(J,11)=CP(5,J+6)
      D(J,12)=CP(5,J+23)
      D(J,14)=CP(6,J+15)
      D(J,16)=CP(7,J+7)
      D(J,17)=CP(7,J+28)
      D(J,19)=CP(8,J+20)
      D(J,21)=CP(9,J+12)
      D(J,22)=CP(9,J+29)
      D(J,23)=CP(10,J)
      D(J,24)=CP(10,J+17)
      IF(J.GT.15) GO TO 50
      D(J,10)=CP(4,J+31)
      IF(J.GT.14) GO TO 50
      D(J+7,8)=CP(4,J)
      D(J+2,13)=CP(6,J)
      IF(J.GT.12) GO TO 50
      D(J+9,20)=CP(9,J)
      IF(J.GT.10) GO TO 50
      D(J,15)=CP(6,J+36)

```

```

IF(J.GT.9) GO TO 50
D(J,20)=CP(8,J+37)
IF(J.GT.8) GO TO 50
D(J,3)=CP(1,J+38)
D(J+8,3)=CP(2,J)
IF(J.GT.7) GO TO 50
D(J,8)=CP(3,J+39)
IF(J.GT.6) GO TO 50
D(J+15,10)=CP(5,J)
D(J+10,15)=CP(7,J)
IF(J.GT.5) GO TO 50
D(J+16,2)=CP(1,J+33)
D(J+16,4)=CP(2,J+25)
D(J+16,6)=CP(3,J+17)
D(J+16,12)=CP(5,J+39)
D(J+16,14)=CP(6,J+31)
D(J+16,16)=CP(7,J+23)
IF(J.GT.4) GO TO 50
D(J+3,25)=CP(10,J+34)
IF(J.GT.3) GO TO 50
D(J+8,25)=CP(10,J+38)
50 D(J+1,18)=CP(8,J)
D(1,13)=CP(5,45)
D(2,13)=CP(5,46)
D(1,18)=CP(7,46)
D(21,1)=CP(1,17)
D(21,3)=CP(2,9)
D(21,5)=CP(3,1)
D(21,7)=CP(3,39)
D(21,9)=CP(4,31)
D(21,11)=CP(5,23)
D(21,13)=CP(6,15)
D(21,15)=CP(7,7)
D(21,17)=CP(7,45)

```

```

D(21,19)=CP(8,37)
D(21,21)=CP(9,29)
D(21,22)=CP(9,46)
D(21,23)=CP(10,17)
D(21,24)=CP(10,34)
D(15,25)=CP(10,42)
D(5,26)=CP(10,43)
D(11,26)=CP(10,44)
D(15,26)=CP(10,45)
RETURN
END
SUBROUTINE WAKE(K,M)

```

```

C
C SUBROUTINE WAKE DEFINES TEMPORARY FIELD POINTS FOR USE IN
C CALCULATING PRESSURE COEFFICIENTS IN THE WAKE REGION.
C
COMMON/FOUR/X0,Y0
XW=X0

C
C DEFINE WAKE BOUNDARY.
C
YW=1.819*(XW**0.926)
IF(Y0.GT.YW) GO TO 10
Y0=YW
10 RETURN
END

```

## REFERENCES

1. Jordinson, R., "Flow in a Jet Directed Normal to the Wind", R.&M. No. 3074, Brit. A.R.C., 1958.
2. Fearn, R. and Weston, R., "Vorticity Associated with a Jet in a Cross Flow", AIAA Journal, Vol. 10, No. 11, Nov. 1972, pp. 1425-1429.
3. Fearn, R. and Weston, R., "Induced Pressure Distribution of a Jet in a Crossflow", NASA TN D-7916, July 1975.
4. Thompson, A.M., "The Flow Induced by Jets Exhausting from a Plane Wall into an Airstream", Ph.D. Thesis, Univ. of London, London, England, Sept. 1971.
5. Bradbury, L.J.S. and Wood, M.N., "The Static Pressure Distribution Around a Circular Jet Exhausting from a Plane Wall into an Airstream", C.P. No. 822, British Aeronautical Research Council, 1965.
6. Wooler, P.T., "Development of an Analytic Model for the Flow of a Jet into a Subsonic Crosswind", NASA SP-218, Sept. 1969.
7. Sellers, W.L., "A Model for the Vortex Pair Associated with a Jet in a Crossflow", Master's Thesis, University of Florida, Gainesville, Florida, March 1975.
8. Batchelor, G.K., "An Introduction to Fluid Dynamics", Cambridge University Press, Cambridge, England, 1967.
9. Chang-Lu, H., "Aufrollung eines Zylindrischen Strahles durch Querwind", Ph.D. Dissertation, Univ. of Gottingen, Gottingen, Germany, 1942.
10. Albertson, M.L., et al., "Diffusion of Submerged Jets", ASCE Transactions, No. 2409, December 1948.
11. Ricou, F.P. and Spaulding, D.B., "Measurements of Entrainment by Axisymmetrical Turbulent Jets", Journal of Fluid Mechanics, 11:21, 1961.
12. Keffer, J.F. and Platten, J.L., "Entrainment in Deflected Axisymmetric Jets at Various Angles to the Stream", University of Toronto, Technical Publication 6808, June 1968.

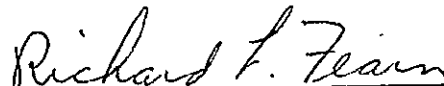


13. Fearn, R., "Mass Entrainment of a Circular Jet in a Cross Flow", NASA SP-218, Sept. 1969.
14. Keffer, J.F., "The Physical Nature of the Subsonic Jet in a Cross-Stream", NASA SP-218, Sept. 1969.
15. Saha, P., "Characteristics of a Round Turbulent Free Jet", Master's Thesis, University of Florida, Gainesville, Florida, March 1975.

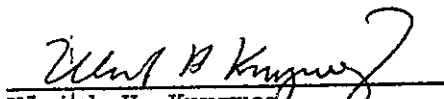
## BIOGRAPHICAL SKETCH

William E. Dietz, Jr. was born in [REDACTED] [REDACTED] on [REDACTED]. After attending schools in Washington, D.C., Japan, and Australia, William graduated from Telopea Park High School in Canberra, Australia in 1970. He entered the Florida Institute of Technology in Melbourne, Florida and received the degree of Bachelor of Science in Mechanical Engineering in June, 1974. He entered the graduate school of the University of Florida and is scheduled to complete the requirements for the degree of Master of Science in Aerospace Engineering in December, 1975.

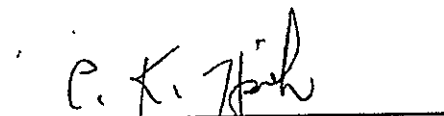
I certify that I have read this study and that in my opinion it conforms to acceptable standards of scholarly presentation and is fully adequate, in scope and quality, as a thesis for the degree of Master of Science in Engineering.

  
Richard L. Fearn, Chairman  
Assistant Professor of  
Engineering Sciences

I certify that I have read this study and that in my opinion it conforms to acceptable standards of scholarly presentation and is fully adequate, in scope and quality, as a thesis for the degree of Master of Science in Engineering.

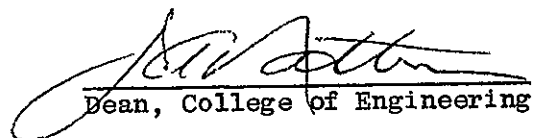
  
Ulrich H. Kurzweg  
Associate Professor of  
Engineering Sciences

I certify that I have read this study and that in my opinion it conforms to acceptable standards of scholarly presentation and is fully adequate, in scope and quality, as a thesis for the degree of Master of Science in Engineering.

  
Chung K. Hsieh  
Associate Professor of  
Mechanical Engineering

This thesis was submitted to the Graduate Faculty of the College of Engineering and to the Graduate Council, and was accepted as partial fulfillment of the requirements for the degree of Master of Science in Engineering.

December, 1975

  
Dean, College of Engineering

\_\_\_\_\_  
Dean, Graduate School